Creep-fatigue deformation behaviour of OFHC-copper and CuCrZr alloy with different heat treatments and with and without neutron irradiation

Singh, Bachu Narain; Li, M.; Stubbins, J.F.; Johansen, B.S.

Publication date:
2005

Document Version
Publisher's PDF, also known as Version of record

RISØ

Risø-R-1528(EN)

Creep-Fatigue Deformation Behaviour of OFHC-Copper and CuCrZr Alloy with Different Heat Treatments and with and without Neutron Irradiation

B.N. Singh, M. Li, J.F. Stubbins and B.S. Johansen

Risø National Laboratory
Roskilde
Denmark
August 2005

Author: B.N. Singh[1)], M. Li[2)], J.F. Stubbins[3)] and B.S. Johansen[1)]
Title: Creep-Fatigue Deformation Behaviour of OFHC-Copper and CuCrZr Alloy with Different Heat Treatments and with and without Neutron Irradiation
Department: Materials Research Department
[1)]Materials Research Department, Risø National Laboratory
DK-4000 Roskilde, Denmark
[2)]Metals and Ceramics Division, Oak Ridge National Laboratory
Oak Ridge, Tennessee, USA
[3)]Department of Nuclear, Plasma and Radiological Engineering
University of Illinois, Urbana, Illinois, USA

Risø-R-1528(EN)
August 2005

Abstract

The creep-fatigue interaction behaviour of a precipitation hardened CuCrZr alloy was investigated at 295 and 573 K. To determine the effect of irradiation a number of fatigue specimens were irradiated at 333 and 573 K to a dose level in the range of 0.2 - 0.3 dpa and were tested at room temperature and 573 K, respectively. The creep-fatigue deformation behaviour of OFHC-copper was also investigated but only in the unirradiated condition and at room temperature. The creep-fatigue interaction was simulated by applying a certain holdtime on both tension and compression sides of the cyclic loading with a frequency of 0.5 Hz. Holdtimes of up to 1000 seconds were used. Creep-fatigue experiments were carried out using strain, load and extension controlled modes of cyclic loading. In addition, a number of "interrupted" creep-fatigue tests were performed on the prime aged CuCuZr specimens in the strain controlled mode with a strain amplitude of 0.5% and a holdtime of 10 seconds. The lifetimes in terms of the number of cycles to failure were determined at different strain and load amplitudes at each holdtime. Post-deformation microstructures was investigated using a transmission electron microscopy.

The main results of these investigations are presented and their implications are briefly discussed in the present report. The central conclusion emerging from the present work is that the application of holdtime generally reduces the number of cycles to failure. The largest reduction was found to be in the case of OFHC-copper. Surprisingly, the magnitude of this reduction is found to be larger at lower levels of strain or stress amplitudes, particularly when the level of the stress amplitude is below the monotonic yield strength of the material. The reduction in the yield strength due to overaging heat treatments causes a substantial decrease in the number of cycles to failure at all holdtimes investigated. The increase in the yield strength due to neutron irradiation at 333 K, on the other hand, causes an increase in the number of cycles to failure. The irradiation at 573 K to a dose level of 0.2-0.3 dpa does not play any significant role in determining the lifetime under creep-fatigue testing conditions.

ISSN 0106-2840
ISBN 87-550-3465-9

Contract no.:
TW1-TVV-COP,
TW2-TVM-CUCFA and
TW3-TVM-CUCFA2

Group's own reg. no.:
1610013-00

Sponsorship:
EU-Fusion Technology Programme

Cover :

Pages: 55
Tables: 4
References: 7

Risø National Laboratory
Information Service Department
P.O.Box 49
DK-4000 Roskilde
Denmark
Telephone +45 46774004
bibl@risoe.dk
Fax +45 46774013
www.risoe.dk

Contents

1 Introduction

Currently, precipitation hardened CuCrZr is the prime candidate for use in the first wall and divertor components of ITER. In service, these components will be exposed to an intense flux of fusion (14 MeV) neutrons and will experience thermo-mechanical cyclic loading as a result of the cyclic nature of plasma burn operations of the system. Consequently, the structural materials in the reactor vessel will have to endure not only the cyclic loading but also the stress relaxation and microstructural recovery (i.e. creep) during the "plasma-on" and "plasma-off" periods. In order to evaluate the impact of this interaction (i.e. creep-fatigue), investigations were initiated to determine the lifetime of the CuCrZr alloy under the conditions of creep-fatigue interaction.

In the present work, the problem of creep-fatigue interaction was investigated by applying a certain holdtime on both tension and compression sides of the cyclic loading. These tests were carried out using strain, load and extension controlled modes of cyclic loading. These tests were performed on a precipitation hardened CuCrZr alloy in the prime aged and overaged conditions. Both unirradiated and neutron irradiated specimens of CuCrZr were tested at room temperature and 573 K with different holdtimes in the range of 0 to 1000 seconds. In addition a number of "interrupted" creep-fatigue tests were carried out at room temperature with a holdtime of 10 seconds. For comparison purposes, a number of tests were performed also on the specimens of annealed OFHC-copper. The results of these investigations are described in section 3 including the results of pre- and post-deformation microstructures obtained using transmission electron microscopy. The analysis and discussion of the results are presented in section 4. Section 5 presents a brief summary and conclusions of the present work. It is appropriate to point out that the results of investigations of the low cycle fatigue (i.e. without holdtime) behaviour of the CuCrZr alloy at different temperatures and the related pre- and post-deformation microstructures in the unirradiated and neutron irradiated conditions have been reported in detail in [1-2]. Results of similar investigations on a dispersion hardened alloy Cu AL 25 are described in Ref.[3].

2 Material and Experimental Procedure

The material used in the present investigations were OFHC-copper and a precipitation hardened copper alloy, CuCrZr. The alloy was supplied by Outokumpu Oyj (Finland) with a composition of Cu – 0.73% Cr – 0.14%. Zr. The alloy was solution annealed at 1233 K for 3 hours, water quenched and then heat treated at 733 K for 3 hours to produce the prime aged (PA) condition. Two further heat treatments were also examined. These were prime aged plus an additional anneal in vacuum at 873 K for 1 hour, referred to as heat treatment 1 (HT1) or for 4 hours, referred to as heat treatment 2 (HT2), and water quenched. Details of the resulting microstructures are given in Table 1. The regular creep-fatigue tests were carried out on cylindrical specimens whereas the "interrupted" tests were performed on rectangular specimens (see Figure 1 for geometry and dimensions).

A number of subsize fatigue specimens of CuCrZr were irradiated with fission neutrons in the BR-2 reactor at Mol (Belgium) at either 333 or 573 K. A number of tensile specimens of CuCrZr with different heat treatments were also irradiated at 333 or 573 K.

The neutron flux during irradiation of tensile specimens was ≈2.5 x 10^{17} n/m^2s (E > 1 MeV) which corresponds to a displacement damage rate of ~5 x 10^{-8} dpa/s (NRT). Specimens received a fluence of ≃1.5 x 10^{24} n/m^2 (E > 1 MeV) corresponding to a displacement dose level of ≃ 0.3 dpa. Fatigue specimens irradiated at 333 or 573 K received a displacement dose in the range of 0.16 to 0.33 dpa at a damage rate in the range of 3-6 x10^{-8} dpa/s (NRT). Details of these irradiations are described in Ref. [4].

Mechanical testing was carried out in an Instron machine with a specially constructed vacuum chamber where the specimen could be gripped and loaded. Tests were conducted in a load-controlled mode in a servo-electrical mechanical test stand. The characteristics of the loading cycles were monitored and controlled by computer. The loading cycles were always fully reversed (i.e. R = -1) so that the maximum tension load was the same as the maximum compressive load. The loading frequency was 0.5 Hz. The creep-fatigue interaction condition was simulated by applying a certain holdtime on both tension and compression sides of the cyclic loading. Holdtimes of up to 1000 seconds were used. The specimens tested with and without holdtimes were cycled to failure, where failure was defined as separation of the specimens into two halves. For a given holdtime, the number of cycles to failure was determined at different stress or strain amplitudes. In addition, one set of specimens were cycled to various portions of the failure life and then sectioned for microstructural examination to determine the evolution of the deformation microstructure as a function of failure life.

The creep-fatigue interaction tests were carried out at 295 and 573 K. For elevated temperature testing, the specimens were heated (in vacuum) by electrical resistance furnaces such that the heat was conducted through the specimen grips. This resulted in an accurate temperature control and no measurable temperature gradient along the specimen length.

Additional creep-fatigue tests were carried out on unirradiated material with all three heat treatments in strain control mode at room temperature. These tests used hold times of 0 or 10 seconds. Further tests were carried out on the prime aged (PA) condition in extension control mode where the load range was continuously monitored between balanced tension and compression limits, but without direct measurement of specimen strain range. These tests were performed on unirradiated CuCrZr PA at room temperature and 523 K.

Following creep-fatigue interaction tests, the post-deformation microstructure was examined by transmission electron microscopy (TEM). 3 mm discs were cut from the gauge sections perpendicular to the creep-fatigue axis. Specimens were taken at a distance from the fracture surface to best represent the stable bulk microstructure prior to failure. The discs were mechanically thinned to ≃0.1 mm and then twin-jet electropolished in a solution of 25% perchloric acid, 25% ethanol and 50% water at 11 V for about 15 seconds at 293 K. The thin foils were examined in a JEOL 2000 FX transmission electron microscope.

3 Experimental Results

3.1 Effect of heat treatment and neutron irradiation on microstructure

In order to understand the mechanical response of the CuCrZr alloy tested under creep-fatigue conditions, it is crucially important to know the details of the microstructural state of the alloy prior to mechanical testing. It is expected that both thermal annealing and neutron irradiation would significantly modify the microstructure and hence the deformation behaviour of CuCrZr alloy. In a previous study, the effect of heat treatments on the precipitate microstructure of the present alloy has been properly characterised [5]. In the following we provide a brief summary of the results relevant to the present investigations.

After each heat treatment, PA, HT1 and HT2, specimens were examined in a transmission electron microscope (TEM) and precipitate size and density were determined. As expected, heat treatments after prime aging (PA) led to a significant coarsening of the prime aged precipitate microstructure. The precipitate size distributions for specimens having received different heat treatments (i.e. PA, HT1 and HT2) are shown in Figure 2. The average precipitate size and density for various heat treatments are quoted in Table 1. The results shown in Figure 2 and Table 1 clearly demonstrates that the overaging heat treatments HT1 and HT2 cause very significant degree of precipitate coarsening. Clearly, caution should be exercised during manufacturing of components for the first wall and diverter components of ITER containing CuCrZr alloy.

Table 1. The average precipitate size and density in CuCrZr alloy after different heat treatments.

Heat Treatment	Precipitate Size (nm)	Precipitate Density (m^{-3})
PA (Prime Aged)	2.2	2.6×10^{23}
PA + 873 K/1 h (HT1)	8.7	1.7×10^{22}
PA + 873 K /4 h (HT2)	21.3	1.5×10^{21}

Microstructures of CuCrZr specimens with heat treatments PA, HT1 and HT2 and neutron irradiated at 333 K to 0.3 dpa were also investigated using transmission electron microscopy [6]. In all three types of specimens (i.e. PA, HT1 and HT2), the microstructure is dominated by high density of irradiation-induced small (2-3nm) vacancy clusters in the form of stacking fault tetrahedra (SFTs). The density, size and

spartial distribution of the irradiation induced SFTs are found to be very similar in the PA, HT1 and HT2 types of specimens. Furthermore, the pre-irradiation precipitate microstructure (i.e. precipitate size, density and spartial distribution) remains largely unaltered during irradiation. Typical examples of the as-irradiated microstructure containing precipitates and SFTs in the PA and HT1 CuCrZr specimens irradiated at 333 K to 0.3 dpa are shown in Figure 3.

3.2 Effect of heat treatment and neutron irradiation on tensile properties

In order to gain some insight into the deformation processes operating during cyclic loading (e.g. fatigue or creep-fatigue) experiments it is necessary to have the knowledge of tensile properties (e.g. yield strength and work hardening behaviour) of the material concerned. In an earlier study, tensile properties of the same CuCrZr alloy as used in the present investigations in the PA, HT1 and HT2 conditions have been investigated both in the unirradiated and irradiated conditions (see [5] for details). The tensile results for different irradiation and testing conditions are summarised in Table 2. All tensile tests were carried out with a strain rate of $1.2*10^{-3}s^{-1}$. While tensile test at lower temperatures (295 K and 333 K) were carried out in air, tests at 573 K were performed in vacuum ($<10^{-7}bar$).

The results presented in Table 2 clearly illustrate the following significant features:

(a) The overaging heat treatments HT1 and HT2 cause a substantial decrease in the yield strength,

(b) Neutron irradiation at 333 K leads to a noticeable increase in the yield strength of the prime aged as well as overaged specimens,

(c) Neutron irradiation at 573 K of the PA as well as the overaged HT1 and HT2 specimens, on the other hand, causes a noticeable decrease in the yield strength.

(d) Neutron irradiation to 0.3 dpa causes a significant decrease in ductility of all three types (i.e. PA, HT1 and HT2) of specimens. The decrease in ductility is rather drastic at the irradiation and testing temperature of 333 K. The post-deformation microstructure suggests that all these materials suffer from the problem of flow localization in the form of cleared channels during post-irradiation testing and this may be responsible for the reduction in ductility.

Table 2. Effect of heat treatments on tensile properties of CuCrZr alloy before and after irradiation at 333 and 573 K to 0.3 dpa

Test No.	Heat Treatment	Irr. Temp. (K)	Dose (dpa)	Test Temp. (K)	$\sigma_{0.2}$ (MPa)	σ_{max} (MPa)	ε_u (%)	ε_t (%)
1225	PA	-	-	323	290.0	398.0	24.0	28.0
1226	”	-	-	323	295.0	416.0	22.0	30.0
1382	”	-	-	333	280.0	373.1	21.3	25.4
1384	“	-	-	“	260.0	364.0	20.0	24.0
1217	HT1	-	-	323	200.0	318.0	26.0	30.0
1211	HT2	-	-	“	175.0	289.0	24.0	32.0
1218	“	-	-	“	165.0	307.0	34.0	41.0
1219	PA	-	-	573	240.0	304.0		
1220	“	-	-	“	250.0	328.0	18.0	27.0
1385	“	-	-	“	244.0	308.0	17.0	23.0
1221	HT1	-	-	573	180.0	255.0	15.0	19.0
1222	“	-	-	“	150.0	227.0	19.0	24.0
1223	HT2	-	-	573	135.0	218.0	17.0	21.0
1224	“	-	-	“	120.0	201.0	22.0	28.0
							25.0	36.0
1360	PA	333	0.3	333	435.0	436.0	2.0	6.0
1353	”	“	“	295	450.0	458.6	1.7	6.8
1354	HT1	“	“	295	410.0	422.2	1.8	9.6
1358	”	“	“	333	397.0	397.0	2.0	15.0
1355	HT2	“	“	295	360.0	363.0	1.4	9.7
1359	”	“	“	333	372.0	372.0	1.0	7.0
1386	PA	573	“	573	210.0	268.0	10.0	12.0
1577	“	“	“	“	190.0	245.0	6.0	8.0
1387	HT1	“	“	573	-	209.0	14.0	18.0
1576	“	“	“	“	134.0	192.0	9.0	12.0
1388	HT2	“	“	573	-	193.0	21.0	27.0
1389	“	“	“	“	119.0	188.0	20.0	26.0

PA: Prime aged.

HT1: PA + 873 K/1 h; HT2: PA + 873 K/4 h.

3.3 Fatigue and ceep-fatigue life as a function of stress amplitude

The variation of the number of cycles to failure, N_f, with the stress amplitude for the prime aged (PA) CuCrZr alloy tested at 295 K and 573 K is shown in Figure 4 (a) for the unirradiated and Figure 4 (b) for the irradiated specimens. Note that the irradiated specimens tested at 295 K were irradiated at 333 K. The specimens tested at 573 K, on the other hand, were also irradiated at 573 K. The displacement dose level reached at both temperatures varied between 0.2 and 0.3 dpa. The results presented in Figures 4 (a) and 4 (b) suggest that the number of cycles to failure, N_f, for the prime aged (PA) CuCrZr alloy tested at 295 K is not very sensitive to the application of holdtime during cyclic loading. The general trend seems to be, however, that the application of holdtime always reduces the number of cycles to failure (at a given stress amplitude). It should be noted that the effect of holdtime on the number of cycles to failure is more marked at the test temperature of 573 K than at 295 K. The effect is even stronger in the case of irradiated specimens. In fact, the largest effect of creep-fatigue mode of cyclic loading on the number of cycles to failure is that of the test temperature both for the unirradiated and irradiated specimens. The irradiation at 333 K of the prime aged CuCrZr alloy tested at 295 K increases the number of cycles to failure (at a given stress amplitude). The irradiation at 573 K and testing at 573 K do not, on the other hand, appear to have any significant effect on the number of cycles to failure.

One of the main objectives of the present work was to examine the impact of overaging heat treatments on the mechanical performance of the CuCrZr alloy. Since the overaging heat treatments at 873 K for 1 and 4 hours (HT1 and HT2, respectively) cause substantial changes in the microstructure as well as tensile properties (see section 3.1 and 3.2), the effects of these heat treatments on the creep-fatigue lifetime was investigated. In the case of heat treatment HT1, the effect of irradiation at 333 K and 573 K was also investigated. The results of creep-fatigue tests with different holdtimes performed at 295 K and 573 K are shown in Figures 5 (a) and 5 (b) for the unirradiated and irradiated conditions. A number of unirradiated CuCrZr specimens with heat treatment HT2 were also tested at 295 K and 573 K with zero and 100 seconds holdtime; the results are shown in Figure 6.

The comparison of results shown in Figure 5 with those in Figure 4 shows that the overall creep-fatigue performance of the overaged CuCrZr specimens with the heat treatment HT1 is very similar to that of the prime aged specimens. There is however, a significant difference in that the number of cycles to failure at a given stress amplitude of the unirradiated specimens with HT1 heat treatment is considerably lower than that of the prime aged specimens both at 295 K and 573 K. The irradiation at 333 K, however, reduces this difference. The irradiation at 573 K, on the other hand, does not lead to such a reduction. In other words, the number of cycles to failure (at a given stress amplitude) for the prime aged specimens remains considerably higher than that obtained for the specimens with HT1 treatment and irradiated and tested at 573 K. The behaviour described above is observed in all the tests carried out with 10 or 100 seconds holdtime.

The specimens of CuCrZr alloy overaged at 873 K for 4 hours (HT2) and tested at 295 K yielded the number of cycles to failure even lower than that observed in the case of specimens given the overaging treatment HT1 (compare Figures 5 and 6). The results also indicate that the effect of 100 seconds holdtime may be more detrimental than 10

seconds holdtime. In order to obtain an overall impression of the effect of various test parameters on fatigue and creep-fatigue behaviour, the number of cycles to failure determined for all specimens tested at room temperature in the load control mode with and without holdtime are shown in Figure 7. These test data include all three heat treatments and values for specimens in the unirradiated and irradiated conditions. The room temperature data for unirradiated CuCrZr fall on two trend curves. The PA condition shows a higher fatigue life than for either of the two overaged conditions, HT1 and HT2. In fact, the values for HT1 and HT2 fall in a similar range. For both the PA and HT1 conditions, the hold time of 10 or 100 seconds have only a marginal effect on life. The values for lives with and without hold periods are nearly the same within typical scatter in the fatigue testing. There is a noticeable difference, however, between the life values for the HT2 condition with and without hold period. In fact, the fatigue life of the HT2 condition with no hold time is better than that for the HT1 condition, while the HT2 condition with 100 seconds hold time has fatigue lives at the lower bound of any of the other conditions tested here.

The irradiated conditions, shown with open symbols in Figure 7, typically show higher fatigue lives than their unirradiated counterparts.

The fatigue and creep-fatigue lifetimes are shown in Figure 8 for specimens tested at 573 K. These test data include heat treatments PA and HT1 in both the unirradiated and irradiated conditions. The 573 K data fall in two trend bands which are related to the heat treatment. The fatigue and creep-fatigue values for the prime aged, PA, condition are shown in the same scatter band both with and without irradiation exposure. The conditions with holdtimes fall at the lower boundary of the band compared to those conditions with no hold. This is true for both irradiated and unirradiated conditions.

Similarly, the results for the HT1 specimens show that they cluster together in a data band similar to, but lower in value than, that for the PA condition. Again, the fatigue lives with no hold are at the upper bound of the band, while the conditions with 10 or 100 seconds holdtime are along the lower bound of the band. Both unirradiated and irradiated materials behave in a very similar manner.

3.4 Fatigue and creep-fatigue life as a function of strain amplitude

Fatigue and fatigue with hold time tests were run in strain control to verify the response with holds at a maximum tension and compression strain points. These data are useful to compare and contrast the effect of hold periods in load control where the maximum stress is constant and the material can strain in creep during the holdtime, and in strain control where stress relaxation occurs at a fixed strain level.

In this section, we first show the results of creep-fatigue tests carried out on OFHC-copper at room temperature in the strain control mode. Figure 9(a) shows the strain amplitude dependence of the number of cycles to failure for no holdtime as well as 10 seconds holdtime. Clearly, the application of holdtime reduces the number of cycles to failure and this reduction becomes progressively worse with decreasing strain amplitude. The separate elastic and plastic portions of the fatigue and creep-fatigue life response are plotted in Figure 9(b). Since the annealed copper is a very weak material, it is not very surprising that at the higher total strain range values, it is the plastic strain range response that dominates the total creep-fatigue performance whereas at the lower

total strain range values, the creep-fatigue performance is dominated by the elastic strain range contribution.

The results of the strain control tests at room temperature are shown in Figure 10 where the numbers of cycles to failure are shown as a function of the total strain amplitude for the three heat treatments (i.e. PA, HT1 and HT2) with and without 10 seconds hold periods. The curves indicate that, under strain control, the fatigue lives of all three heat treatment conditions are very similar. The inclusion of a hold period in maximum tension and compression of 10 seconds results in lower fatigue lives. Again, the level of reduction in fatigue lives with a 10 seconds holde period is essentially the same for all heat treatment conditions.

Figure 11 shows the fatigue lives as a function of the strain range for each of the heat treatment conditions where the elastic and plastic components of the total strain range are individually plotted. These comparisons show that the elastic portion of the strain range is much more dominant in terms of the fraction of total strain for the PA condition than for the overaged conditions. This is a reflection of the higher strength in the PA condition. It should be noted that the transition life, that is the point where the elastic and plastic portions of the total strain are equivalent is around a failure life of around 2000 cycles for the PA condition, but greater than 10,000 cycles for the HT2 condition. This is also consistent with the lower strength of the material following overaging.

3.5 Fatigue and creep-fatigue life in balanced load, extension controlled tests

Fatigue and fatigue with hold time tests were performed under total extension control at room temperature and 523 K on the prime aged (PA) CuCrZr. These tests showed balance load (stress) cycles even though direct measurement of specimen strain was not possible. Thus the fatigue life data are reported as a function of stress amplitude. These tests have the advantage over the load control tests (see Section 3.3) that the stresses are balanced around zero mean strain (or extension). In the load-controlled test, the specimen extends (or ratchets) during the tension part of the cycle and the specimen will eventually develop an increasingly large mean strain during cycling. In general, the development of a mean strain, particularly in tension, will have a detrimental effect on fatigue life. For this reason, it is important to also consider the balanced load test results.

The failure lives for all of the hold time conditions are shown as a function of the stress amplitude in Figure 12. No distinction is made for the length of each hold period in these results, though hold periods as short as 2 seconds and as long as 1000 seconds are represented in the data. The results for both room temperature and 523 K tests are shown in the figure, and as is expected from the differences in the material strength, the lives for the room temperature conditions are longer at a given stress amplitude.

The effect of hold period on fatigue life is shown in Figure 13 for the same set of experiments. In this case the fatigue failure life is shown as a function of hold period. Four separate sets of data are shown. Two of the four are for representing the room temperature test results at short lives (LCF – low cycle fatigue) which are clustered between 10 and 100 cycles to failure in Figure 12 and for longer fatigue lives (HCF – high cycle fatigue) clustered around failure lives of about 1000 cycles in Figure 12. Two similar sets of data are also shown for the 523 K tests to the same two types of failure lives. Despite the marginal differences in the actual stress levels for samples in each of

the data sets (see Figure 12), there is little or no effect of hold period on failure life. This is a remarkable result since hold times of as short as 2 seconds have an effect which is similar to holds as long as 1000 seconds. This is found at room temperature, where such a result might be expected due to the limited thermal activation for stress relaxation, but also at 523 K, where thermally activated stress relaxation would be expected. In fact, it is the stress relaxation which is found to occur at both temperatures, but occurs very quickly so that most of the relaxation occurs in less than 2 seconds accounting for the negligible dependence of fatigue life on hold time beyond that time.

3.6 Interrupted creep-fatigue tests

In addition to the regular creep-fatigue tests to failure, a number of "interrupted" creep-fatigue tests were performed on the prime aged CuCrZr alloy at room temperature. It is important to note here that the standard prime aging heat treatment (as defined in section 2) of the specimens used in these tests may not have exactly the same precipitate microstructure as in the regular fatigue specimens because of the differences in the size and geometry between these two types of specimens (see Figures 1(a) and 1(b)). Consequently, the tensile properties of the prime aged used in the regular creep-fatigue tests may be some what different from those of the specimens used in the "interrupted" tests. This difference may ultimately lead to some differences in the hardening/softening behaviour between these two types of CuCrZr specimens during creep-fatigue tests carried out even at the same temperature and strain amplitude level.

The interrupted tests were carried out in strain controlled mode with a strain amplitude of 0.5% and with a tension and compression holdtime of 10 seconds. A number of unirradiated specimens were tested for 1, 2, 5, 25, 100 and 500 cycles. After a given number of cycles, the specimens was unloaded for the microstructural examination (see section 3.7). The evolution of stress in these specimens as a function of the number of cycles is shown in Figure 14. Figure 14 shows that the magnitude of stress decreases with increasing number of cycles, indicating dynamic recovery of the microstructure. The results of microstructural investigations on these specimens are described in the following section (3.7).

3.7 Post-deformation microstructure

The development of microstructure during cyclic loading is of particular interest to understand fatigue performance, particularly since the evolution of fatigue damage will be dependent on the starting microstructure. To examine this issue in greater detail, a series of fatigue tests were interrupted at various points in the fatigue life so that the progression of microstructural development could be examined. The surface of the creep-fatigue tested specimens were investigated using a scanning electron microscopy (SEM) for the appearance of slip steps as a function of the number of creep-fatigue cycles. Figure 15 shows the SEM micrographs illustrating the evolution of slip steps on the surface of the deformed specimens to (a)1,(b) 25 and (c) 500 cycles. As can be seen in Figure 15(a), the slip steps appear already at the end of the first cycle. The number increases with increasing number of cycles. Already at 500 cycles, a well defined crack can be seen at the surface (Figure 15c). At this strain amplitude of 0.5%, the specimen fractured after about 3000 cycles.

Thin foils were prepared for TEM investigations of the evolution of dislocation microstructure as a function of number of cycles. Figure 16 (a-f) shows representative micrographs for specimens creep-fatigue tested to (a)1,(b)2,(c)5,(d)25,(e)100 and (f)500 cycles. Figure 16(a) illustrates that already during the first creep-fatigue cycle, a high density of dislocations are generated. Furthermore, it can be also seen that dislocations already have started to form cell-like structure. With increasing number of cycles this cell-like structure develops into well defined cell walls and cell structure (e.g. Figure 16(c)). At still higher number of cycles, the cell walls become thicker, cell size increases (Figures 16(d) - (e)) and density of free dislocations decreases significantly. By the end of 500 cycles it seems that dislocation density even in the cell walls has decreased drastically and it could be that the cell walls have polygonised into some kind of low angle boundaries.

In order to gain insight into the final deformation processes operative during creep-fatigue interaction tests, thin foils were prepared from specimens that had fractured during these tests under different conditions and were examined in a transmission electron microscope (TEM). These foils were prepared from materials taken from the region in the specimen gauge section, but remote from the point of failure. This is necessary in load controlled tests since some amount of necking and excessive deformation are expected to occur at the point of failure. Samples remote from the failure point may contain more of the actual fatigue-induced microstructure. In spite of this precaution, the TEM examinations of the specimens fatigued (no holdtime) and creep-fatigued (with holdtime) to the end of life (i.e. to fracture) did not yield very useful information regarding the evolution of dislocation microstructure during these tests. Practically all specimens examined showed very similar dislocation microstructure, making it almost impossible to discern any clear effect of the test parameters used on the evolution of the dislocation microstructure. It is worth pointing out, however, that the high density of precipitates (due to aging) and the irradiation induced defect clusters remained homogeneously distributed even at the end of the creep-fatigue tests. An example of the precipitates and defect clusters observed in a prime aged CuCrZr specimen irradiated to ~0.3 dpa at 333 K and tested at 295 K to the end of life (N_f=1200) with a holdtime of 100 seconds and stress amplitude of 350 MPa is shown in Figure 17. The microstructure is similar to the as-irradiated microstructure (prior to deformation) shown in Figure 3(a).

As regards the effect of irradiation on the evolution of dislocation microstructure during post-irradiation deformation, the specimens irradiated at 333 K and tested at 295 K with no holdtime and the holdtime of 100 seconds showed very high density of homogeneously distributed dislocations. Both the prime aged and overaged specimens exhibited very similar microstructure and effect of holdtime or stress amplitude could not be resolved. It is interesting to note, however, that in the irradiated specimens although a large number of dislocations were generated during the cyclic loading, the dislocations were unable to perform long distance transport. As a results, dislocation-dislocation interaction and thereby segregation of dislocations in the form of dislocation walls and cell-like structure did not evolve.

In the specimens irradiated and tested at 573 K, dislocation density was low enough to resolve them clearly in the TEM. Some typical examples of the observed dislocation microstructures in the irradiated and deformed specimens of the prime aged (PA) and overaged (HT1) CuCrZr are shown in Figures 18 and 19, respectively. The results are shown for tests carried out with no holdtime and with the holdtime of 100 seconds. It can

be seen in Figures 18 and 19 that in all cases dislocations are found to be distributed predominantly in a homogeneous fashion. In other words, there is no indication of any significant degree of dislocation segregation in the form of dislocation walls and cell-like structure. There is, however, some indication of some limited amount of dislocation segregation both in the prime aged and the overaged specimens tested without holdtime (see Figures 18a and 19a). However, no such segregation were seen in the corresponding specimens tested with a holdtime of 100 seconds. Furthermore, the dislocation microstructures in specimens tested with a holdtime of 100 seconds appear to be in somewhat recovered state (Figures 18(b) and 19(b)) compared to those in specimens tested with no holdtime (Figures 18(a) and 19(a)).

4 Discussion

4.1 Comparison of load and strain control fatigue behaviour

Three sets of fatigue experiments were performed in this study, each under a different mode of loading condition. It is important to understand the differences and similarities in the fatigue life response for each of these conditions. The majority of the tests were conducted in load control so the standard basis of comparison would be the stress amplitude. For the balanced load, extension controlled tests (Section 3.5), the results are already in the form of the cyclic stress amplitude. For the strain control tests, the stress amplitude changes with cycling (discussed further below in Section 4.3). A usual basis of comparison for stress amplitude is the value of the stress amplitude at half-life. At this point in the fatigue life, the stress response is usually stabilized from any initial hardening or softening behaviour, and is still sufficiently far from the development of a major crack that cycles are typical of stable bulk materials response. The half-life stress amplitudes were measured for the strain control tests reported in Section 3.4.

A comparison of the fatigue failure lives as a function of the stress amplitude for the three test conditions examined in this study are shown in Figure 20. The data for comparison include unirradiated tests run at room temperature, so only these results are shown in the figure. The failure lives are reasonably consistent across test types with some distinctive differences which provide insight into the differences between these three types of tests.

The first major point, however, is that the influence of heat treatment condition can be clearly seen from the results. In all cases, the prime aged, PA, condition shows the highest stress amplitude values at a given life. This is consistent with the higher strength of that condition compared to the two overaged conditions, HT1 and HT2. The second major conclusion from the combined data is that the hold time has a smaller effect on the life versus stress amplitude than does the heat treatment condition. In all cases, the hold time lives are less than those in pure fatigue, but these differences are smaller than the influence of overaging, HT1 and HT2, compared to the prime aged, PA, condition.

When comparing the three different types of test conditions, the PA condition shows the highest strength with the results for the extension controlled tests (see Section 3.5) and the strain controlled tests (see Section 3.4) marginally higher than those for the load controlled tests. This result is consistent with the more aggressive nature of the load control test method where the specimen can incrementally strain to higher and higher mean strains as the test proceeds. Since holds are performed in stress control, the

material strains as much as it can during the hold period. This is particularly damaging in tension stress hold since the material will creep at a constant stress for the entire period of the hold time. This means that the specimen will extend during this period to produce an elongated specimen with mean strain. This is compared to both the strain control and the extension control tests where the specimen is cycled around a balanced strain cycle with zero mean strain and no excessive specimen deformation. In these cases, the stress relaxes at the maximum strain levels at a fixed specimen extension. This avoids specimen ratchetting the development of mean specimen strains.

The results for the load control tests for the HT1 and HT2 specimens show similar results. The load control tests are moderately more aggressive than either strain control or extension control.

4.2 The influence of tensile properties on load and strain control fatigue behaviour

It is informative to consider the influence of the differences in yield strength in the various heat treatment conditions on the fatigue response. There are major differences between yield strength in the PA condition and the HT1 and HT2 conditions at room temperature in the unirradiated condition. Irradiation exposure results in very large increases in the room temperature yield strengths, as seen by the data for the PA and HT1 conditions (see Section 3.2). The influence of the yield strength on the fatigue behaviour is also seen in Figure 11 where the relative level of the elastic strain range is based on material yield strength. For higher yield strength materials, for instance the PA condition here, the elastic contribution to total strain is higher, shifting the transition life to lower fatigue lives. For lower yield strengths, for instance the HT2 condition, the elastic contribution to total strain is less and the transition life is at a higher fatigue life.

To fully appreciate the influence of yield strength on the fatigue performance, the stress amplitude values were normalized with respect to yield strength. The results are shown in Figure 21 where it is seen that all of the fatigue life data for the unirradiated data fall within a band. Only the CuCrZr HT2, pure fatigue data fall above the band. A more remarkable result is found for the irradiated data where all of the data fall on the same trend line (see Figure 21). The explanation of the single line for the irradiated data follows from the fact that the initial stresses in fatigue loading are all below the material yield point (i.e. apart from very short lives, values of less than 1 on the y-axis). This means that the elastic portion dominates in the strain range. In the case of the unirradiated material, the differences in the yield strength account for much of the difference in loading conditions to produce the same failure life, so it is also reasonable that those data fall within the same band. The only outlier in that band is the HT2 condition which has the lowest yield strength and the highest relative ductility in those conditions, and thus the largest plastic strain amplitude. Though direct measurements of the elastic and plastic strain amplitudes could not be made for the load controlled tests, this should account for the behaviour of the HT2 condition.

Even a more clear demonstration of the effect of yield strength on fatigue and creep-fatigue deformation behaviour of OFHC-copper and CuCrZr alloy in the PA, HT1 and HT2 conditions is presented in Figure 22. Here the lifetime (N_f) results obtained in the strain controlled tests carried out at 295 K are shown as a function of stress amplitude.

The yield strength ($\sigma_{0.2}$) values for different materials tested are also indicated in the figure. It can be readily seen that the stress amplitude at a given number of cycles to failure (N_f) decreases strongly with decreasing yield strength. It should be also noted that the lifetime of materials with high yield strength (i.e. CuCrZr PA and HT1) is not sensitive to holdtime used in the creep-fatigue tests whereas the holdtime causes a noticeable reduction in the lifetime (N_f) of materials with lower yield strength (i.e.CuCrZr HT2 and OFHC-Cu).

In order to get further insight into the role of yield stress in the evolution of creep-fatigue deformation behaviour, the results shown in Figure 22 are replotted in Figure 23 after normalizing the stress amplitude values with respect to the yield strength ($\sigma_{0.2}$) of OFHC-Cu, and CuCrZr alloy in the prime aged (PA) and overaged (HT1 and HT2) conditions. It is interesting to note that the results for OFHC-Cu and the CuCrZr alloy (Figure 23) are found to fall in two distinctly separated blocks, indicating that the deformation processes controlling the lifetime of OFHC-Cu and CuCrZr alloy must be significantly different. The OFHC-Cu, for instance, survives 10^4 cycles even when the stress amplitude is almost twice the yield strength of OFHC-Cu (Figure 23). The CuCrZr specimens with different heat treatments, on the other hand, reach a lifetime (N_f) of 10^4 cycles at a much lower stress amplitude relative to their yield strength (i.e. at or below the level of the yield strength). It is interesting to note that although the lifetime (N_f) response of the CuCrZr HT2 and OFHC-Cu considered in terms of the stress amplitude alone appears to be very similar (see Figure 22), the same two materials exhibit the largest difference in the lifetime response when considered in terms of the relative stress amplitude in Figure 23. Furthermore, although there are big differences in the yield strength of CuCrZr alloy with different heat treatments (i.e. PA, HT1 and HT2), the lifetime response considered in terms of the relative stress amplitude in Figure 23, does not show any significant differences in the response of PA, HT1 and HT2. It is also worth noting that most of the CuCrZr specimens containing precipitates fail at stress amplitudes below their yield strength. In view of the lack of microstructural information, it is rather difficult to interpret these results in terms of the role of the precipitates on the evolution of dislocation microstructure under these conditions. Nonetheless, it seems very likely that it must be the precipitate microstructure that interferes with dislocation dynamics and possibly causes the localization of strains which might, in the end, be responsible for crack nucleation.

The fatigue lives as a function of the stress amplitude normalized with respect to the yield strength are shown in Figure 24 for the 573 K data. It is noteworthy in this cases that all of the pure fatigue for the unirradiated and irradiated cases fall on two separate lines, as do the unirradiated and irradiated hold time data. In these cases, the loading stresses were always in excess of the yields strengths (i.e. stress amplitude/yield strength values greater than one) so plastic strain levels would be significant. Also, because of this and ratcheting effects, the influence of the hold period on fatigue life would produce shorter fatigue lives as shown. Note also that, at this temperature, the influence of irradiation exposure on tensile properties and fatigue lives is small.

4.3 Cyclic hardening and softening behaviour under fatigue loading

The stability of the stress and strain during fatigue cycling provides an indication of the stability of the microstructure during loading history. The maximum tensile stress as a

function of fatigue cycles are shown in Figure 25 for (a) OFHC-Cu, and CuCrZr alloy in (b) PA, (c) HT1 and (d) HT2 conditions. All specimens were tested at 295 K in the strain control mode. It can be easily seen in Figure 25(a) that OFHC-Cu first hardens with increasing number of cycles and then reaches a stable stress level and remains at that level until the end of life. It should be noted that the hardening rate and the magnitude of hardening increase with increasing strain amplitude. The PA condition first hardens with life, and then softens. The HT1 condition shows an initial hardening followed by a stable stress level through the life. Finally HT2 shows a steady softening behaviour through cyclic life with a plateau in stress amplitude toward the end of life.

This tendency for cyclic hardening or softening can also be observed in the load control tests where the area of the nominal fatigue loop was monitored during the fatigue cycling period. The nominal strain was measured with an LVDT which provides good qualitative insight into the stress-strain behaviour, but without accurate quantitative strain values. Four conditions are shown for the prime aged (PA) CuCrZr room temperature tests with and without irradiation in Figure 26 and CuCrZr at 573 K with and without irradiation in Figure 27. Results of similar tests carried out on the overaged (HT1) CuCrZr specimens in the (a) unirradiated and (b) irradiated conditions are showen in Figure 28 and 29, respectively. The general hardening trend can be seen for the unirradited material by the decrease in fatigue loop size. This is followed by a stable loop size for most of the life, and finally a loop broadening which is an indication of severe plastic deformation at the end of life. The irradiated material at room temperature shows an initially small loop size which is a good indication that the material is being loaded below its yield strength (see also Figure 21). However, as cycling continues, the material gradually softens to produce larger loop areas. This is presumably due to dislocation interactions with existing irradiation-induced defects, some of which are eventually wiped away by the cycling to produce a more ductile microstructure.

4.4 The influence of heat treatment and holdtime on fatigue life

A major issue for study in this program was the influence of heat treatment and hold time on the fatigue performance of CuCrZr. The heat treatment effects are shown to be distinctively based, to a large extent, on the differences in yields strength, but to some degree also on the differences in response to cyclic softening and hardening as is shown in Figure 25.

The influence of hold time was found to be relatively small for many of the conditions shown here. There is a clear influence in the load controlled tests where creep-ratcheting is a consequence of holds in the load control tests. In most cases, the loading conditions were severe and resulted in lives of less than 10,000 cycles to failure. It is noteworthy, however, that in the strain controlled tests at room temperature, the biggest effect of hold period was for the lowest strain ranges or the longest lives, precisely the conditions of most design interest. The current work cannot provide a clear explanation for this observation which deserves further study, particularly because of its potential impact on design decisions.

5 Summary and Conclusions

The present report describes the main findings of a systematic study of the creep-fatigue interaction behaviour of a precipitation hardened CuCrZr alloy in the prime aged (PA)

condition and with two overaging heat treatments (HT1 and HT2). For comparison purposes, a limited number of creep-fatigue experiments were also carried out on fully annealed OFHC-copper specimens in the unirradiated condition. In the present work, the creep-fatigue interaction was simulated by applying a certain holdtime on both tension and compression sides of the cyclic loading procedure. The effect of different holdtimes of 0, 10 and 100 seconds on the lifetime and the number of cycles to failure was investigated at 295 K and 573 K. Most tests were run with load-control conditions and others were run in strain control mode. A number of CuCrZr specimens irradiated at either 333K or 573K to a displacement dose level in the range of 0.16-0.33 dpa (NRT) were also tested at room temperature or 573 K, respectively, with different holdtimes and stress amplitude levels. In addition to determining the mechanical response under creep-fatigue testing, the post-deformation microstructure was investigated using TEM, including a series of interrupted tests where the development of the fatigue-induced microstructure was examined as a function of the fraction of fatigue life.

On the basis of the results reported here, the following preliminary conclusions can be drawn:

(i) The overaging heat treatments have strong effect on the fatigue and creep-fatigue performance and lifetime of the CuCrZr alloy. The effect arises primarily because of the decrease in the yield strength due to overaging.

(ii) The yield strength of the material plays a complicated role in determining the fatigue and creep-fatigue lifetime. The higher the yield strength, the longer is the lifetime at a given stress/strain amplitude.

(iii) The analysis of the lifetime of OFHC-Cu and CuCrZr alloy tested in strain control mode in terms of the normalized stress amplitude suggests that the dense population of precipitates in the CuCrZr alloy is likely to restrict dislocation motion and may cause dislocation segregation and strain localization which in turn may lead to crack nucleation. This effect may get further intensified in the irradiated specimens because of the presence of irradiation induced defects and their clusters.

(iv) The effect of holdtime on creep-fatigue life is not very significant. However, the application of holdtime practically always reduces the number of cycles to failure. The effect of holdtime appears to be complicated and seems to depend on a number of variables such as stress/strain amplitude, the mode of cyclic loading, the yield strength of the material, etc. The fact that the reduction in creep-fatigue lifetime increases with decreasing stress/strain amplitude is a matter of concern because the origin of this effect is not at all understood.

(v) The irradiation of both prime aged (PA) and overaged (HT1) CuCrZr specimens at 333 K to 0.3 dpa causes an increase in the number of cycles to failure (at a given stress amplitude) when tested at 295 K. This increase is most probably due to a large increase in the yield strength caused by irradiation. The irradiation at 573 K, on the other hand, does not appear to have any significant effect on the number of cycles to failure.

(vi) Test temperature both in the case of irradiated and unirradiated specimens has a strong effect on the creep-fatigue lifetime.

At this point in time, the effect of holdtime on the mechanical performance and the lifetime of the CuCrZr alloy used in the present work remains rather elusive. Even the post-deformation microstructural evidence and the features of the fracture surfaces do not help much in identifying the physical process(es) controlling the lifetime and the number of cycles to failure under the creep-fatigue testing conditions. A considerable amount of additional work is deemed necessary to establish a proper understanding of the process(es) controlling the effect of holdtime. However, at this juncture we may speculate in terms of qualitative and empirical arguments that the origin of the effect may lie in the nucleation of cracks during the holdtime and their subsequent healing and growth during the relaxation periods both on the tension and compression sides of the cyclic loading. According to this argument, high strain amplitudes, high temperatures and long holdtimes would be expected to contribute significantly to crack-tip blunting and crack healing. In contrast, no such beneficial effect can be expected at low strain amplitudes, low holdtimes, and low temperatures.

Acknowledgements

The present work was partly funded by the European Fusion Technology Programme. The authors would like to express their gratitude to Drs. Jean Dekeyser and Patrice Jacquet for organizing irradiations in the BR-2 reactor at Mol (Belgium). The authors would like to thank B.F. Olsen, N.J. Pedersen and G. Christiansen at Risø and X. Wu and X. Pan at the University of Illinois for the technical assistance.

References

[1] B.N. Singh, J.F. Stubbins and P. Toft. Risø Report No. Risø-R-991(EN), May (1997), 42 p.

[2] B.N. Singh, J.F. Stubbins and P. Toft. Risø Report No. Risø-R-1128(EN), March (2000), 55 p.

[3] B.N. Singh, J.F. Stubbins and P. Toft, J. Nucl. Mater. 275 (1999), 125.

[4] P. Jacquet, SCK-CEN Report No. SCK-CEN-R-3732, June (2003), 50 p.

[5] B.N. Singh, D.J. Edwards and S. Tähtinen, Risø Report No. Risø-R-1436(EN), December (2004), 24 p.

[6] D.J. Edwards and B.N. Singh, to be published.

[7] B.N. Singh, D.J. Edwards and P. Toft, J. Nucl. Mater. 238 (1996) 244.

Appendix

The following Tables list the raw results of different types of creep-fatigue tests carried out on CuCrZr alloy with different heat treatments tested both in unirradiated and neutron irradiation conditions. Some results on fully annealed OFHC-copper tested at 295 K in the unirradiated condition in strain controlled mode, are also included.

Table A1. Strain controlled creep- fatigue tests.

Material	Heat Treat -ment	Dose (dpa)	Irr. Temp. (K)	Test Temp. (K)	Hold Time (s)	Strain Amplitude			Cycles to Failure (N_f)
						Total (%)	Plastic (%)	Elastic (%)	
OFHC-Cu	Ann.	0	-	295	0	0.10	0.025	0.075	168576
	”	0	-	”	0	0.10	0.025	0.075	158208
	”	0	-	”	0	0.15	0.061	0.089	62734
	“	0	-	“	0	0.20	0.092	0.108	31000
	“	0	-	“	0	0.25	0.130	0.120	13481
	“	0	-	“	10	0.15	0.067	0.083	32768
	“	0	-	“	10	0.20	0.102	0.098	17920
	“	0	-	“	10	0.25	0.141	0.109	13888
CuCrZr Outokumpu	PA	0	-	295	0	0.20	0.018	0.182	39752
	”	0	-	”	0	0.20	0.013	0.187	26581
	”	0	-	”	0	0.25	0.043	0.208	24576
	“	0	-	“	0	0.30	0.077	0.223	18944
	“	0	-	“	0	0.40	0.133	0.267	6912
	“	0	-	“	0	0.50	0.239	0.261	3920
	“	0	-	“	0	0.70	0.412	0.288	1100
	“	0	-	“	10	0.20	0.013	0.187	23296
	”	0	-	”	10	0.25	0.044	0.207	17644
	”	0	-	”	10	0.30	0.082	0.219	8300
	“	0	-	“	10	0.40	0.151	0.249	5376
	“	0	-	“	10	0.50	0.248	0.252	3104
	“	0	-	“	10	0.70	0.418	0.282	930
	“	0	-	“	10	0.20	0.016	0.184	36704
	“	0	-	“	10	0.30	0.075	0.225	6492
	“	0	-	“	10	0.50	0.239	0.261	2560
	“	0	-	“	10	0.20	0.016	0.184	33221
	“	0	-	“	10	0.30	0.073	0.227	7624
	“	0	-	”	10	0.50	0.252	0.248	2384

CuCrZr Outokumpu	HT1	0	-	295	0	0.20	0.031	0.169	25216
	”	0	-	”	0	0.30	0.124	0.176	12288
	”	0	-	”	0	0.40	0.200	0.200	6016
	“	0	-	“	0	0.50	0.291	0.209	4290
	“	0	-	“	10	0.20	0.042	0.158	34304
	”	0	-	“	10	0.30	0.117	0.183	11840
	”	0	-	“	10	0.40	0.223	0.177	4288
	“	0	-	“	10	0.40	0.210	0.190	4440
	“	0	-	”	10	0.50	0.304	0.196	2560
	“	0	-	”	10	0.50	0.313	0.187	4064
CuCrZr Outokumpu	HT2	0	-	295	0	0.20	0.076	0.124	43390
	”	0	-	”	0	0.30	0.160	0.140	16960
	”	0	-	”	0	0.40	0.250	1.150	7616
	“	0	-	“	10	0.20	0.086	0.114	26688
	“	0	-	“	10	0.30	0.169	0.131	11008
	“	0	-	“	10	0.40	0.264	0.136	5504

Table A2. Load controlled creep-fatigue tests on CuCrZr (Outokumpu) alloy.

Heat Treatment	Dose (dpa)	Irr. Temp (K)	Test Temp (K)	Hold Time (s)	Stress amplitude (MPa)	Cycles to Failure (N_f)
PA	0	-	295	0	293.5	7420
”	0	-	”	0	310.5	1520
”	0	-	”	0	322	4200
“	0	-	“	0	333.5	2742
“	0	-	“	0	362	346
“	0	-	“	0	362.5	195
“	0	-	“	0	365	235
“	0	-	“	0	367.5	970
PA	0	-	295	10	281.5	4550
”	0	-	”	10	300	4450
”	0	-	”	10	306.5	2470
“	0	-	“	10	333	670
“	0	-	“	10	337.5	2180
“	0	-	“	10	362	150
“	0	-	“	10	367.5	40
“	0	-	“	10	382.5	20
”	0	-	”	10	382.5	20
”	0	-	”	10	410	159
“	0	-	“	10	474.5	7
“	0	-	“	100	347	70
PA	0.18	333	295	0	299	3750
”	0.25	”	”	0	318	2290
”	0.33	”	”	0	341	1010
“	0.33	“	“	10	323	2700
“	0.33	“	“	10	342	355
“	0.33	“	“	10	352.5	190
“	0.33	“	“	10	352.5	170
“	0.33	“	“	100	305.5	450
”	0.25	”	”	100	316.5	3420

”	0.33	”	”	100	317.5	360
“	0.18	“	“	100	376.5	510
“	0.16	“	“	100	411	160
“	0.16	473	“	10	322.5	1170
“	0.16	“	“	100	348	1220
PA	0	-	573	0	214.5	6000+
”	0	-	”	0	252.5	7400
”	0	-	”	0	272	250
“	0	-	“	0	290	70
“	0	-	“	10	257.5	1020
“	0	-	“	10	283.5	58
“	0	-	“	10	326	6
“	0	-	“	100	246.5	380
“	0	-	“	100	262.5	110
“	0	-	“	100	272.5	60
PA	0.3	573	573	0	256.5	3000
”	0.3	”	”	0	269	590
”	0.3	”	”	0	292.5	68
“	0.3	“	“	100	223.5	890
“	0.3	“	“	100	246	700
“	0.3	“	“	100	259	48
HT1	0	-	295	0	199	9500
”	0	-	”	0	244	1610
”	0	-	”	0	259	825
“	0	-	“	0	290	330
“	0	-	“	0	290	250
“	0	-	“	0	300	9
“	0	-	“	0	300	50
”	0	-	“	0	300	178
”	0	-	“	10	202.5	3800
“	0	-	”	10	226	1610
“	0	-	”	10	226	2360
“	0	-	”	10	246.5	240
“	0	-	”	10	279	132
”	0	-	”	100	232.5	975

”	0	-	”	100	239	650
“	0	-	“	100	252.5	250
“	0	-	”	100	272.5	79
“	0	-	”	100	299	9
HT1	0	-	573	0	160	5130
”	0	-	”	0	171	1955
”	0	-	”	0	184	635
”	0	-	“	10	165	770
“	0	-	“	10	176.5	330
“	0	-	“	10	194.5	35
“	0	-	“	100	163.5	980
HT1	0.28	333	295	0	275	2835
”	0.33	”	”	0	319	380
”	0.28	”	”	0	320	705
”	0.28	”	”	0	325	240
“	0.33	“	“	0	345	100
“	0.25	“	“	0	410	9
“	0.16	“	“	10	279	1140
“	0.16	“	“	10	324.5	170
”	0.25	”	”	10	326	150
”	0.16	”	”	10	348.5	50
“	0.25	“	“	10	405	6
“	0.28	“	“	100	276.5	1230
“	0.28	“	“	100	325.5	165
“	0.28	“	“	100	352	50
HT1	0.3	573	573	0	169	9000
”	”	”	”	0	195	390
”	”	”	”	0	220	100
”	”	“	“	10	181	220
“	“	“	“	10	192.5	118
“	“	“	“	100	162.5	1400
“	“	“	“	100	167	500
“	“	“	“	100	183.5	120
“	“	“	“	100	196.5	33

HT2	0	-	295	0	207.5	2850
”	0	-	”	0	235	1050
”	0	-	”	0	259	130
“	0	-	“	0	265	278
“	0	-	“	0	268	75
“	0	-	“	0	270	240
”	0	-	”	0	277	36
”	0	-	”	100	177	2400
“	0	-	“	100	180	1900
“	0	-	“	100	187.5	1820
“	0	-	“	100	187.5	3500
”	0	-	”	100	203.5	2500
”	0	-	”	100	227.5	520
“	0	-	“	100	247.5	190
“	0	-	“	100	257	25
“	0	-	“	100	261	23
“	0	-	“	100	271.5	11
“	0	-	“	100	271.5	13
“	0	-	“	100	272.5	50
HT2	0	-	573	0	137	13950
”	0	-	”	0	147	2775
”	0	-	”	0	176	208
“	0	-	“	0	200	48
”	0	-	“	100	140	1580
”	0	-	“	100	168	80
“	0	-	”	100	179	24
“	0	-	“	100	189	4

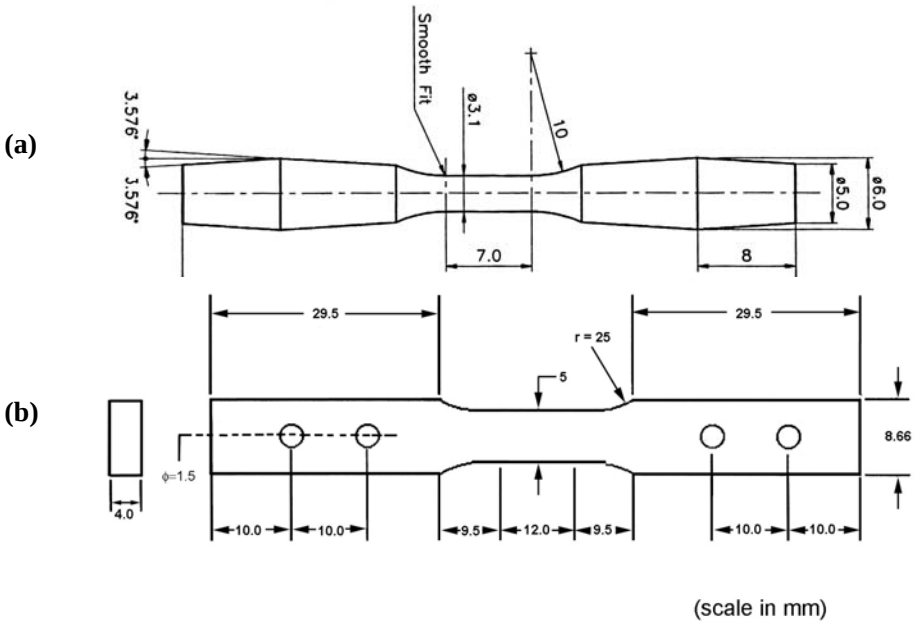

Figure 1. Geometry and dimensions of fatigue specimens (a) for regular fatigue and creep-fatigue tests and (b) for "interrupted" creep-fatigue tests.

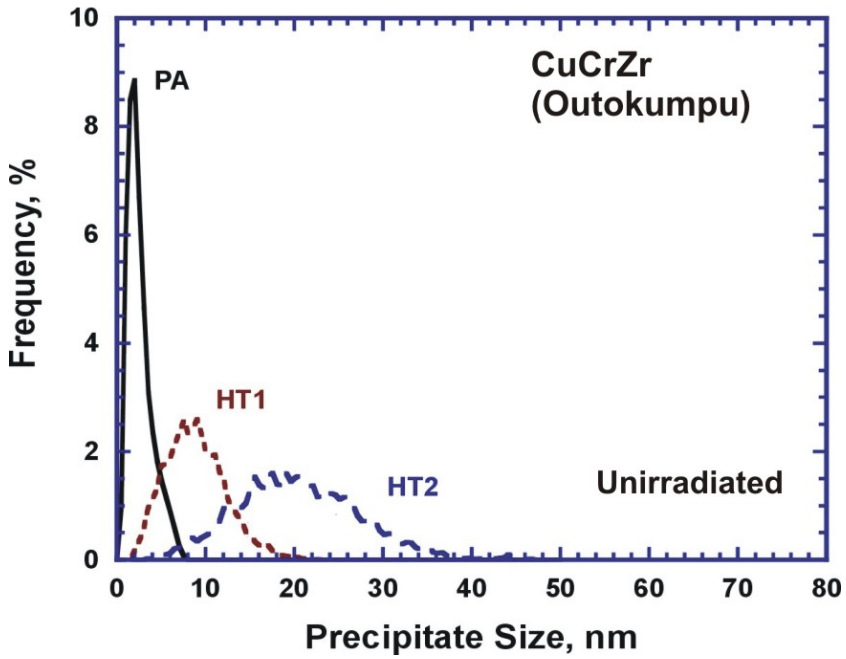

Figure 2. Precipitate size distributions for Outokumpu CuCrZr alloy in the prime aged (PA) and overaged (HT1 and HT2) conditions.

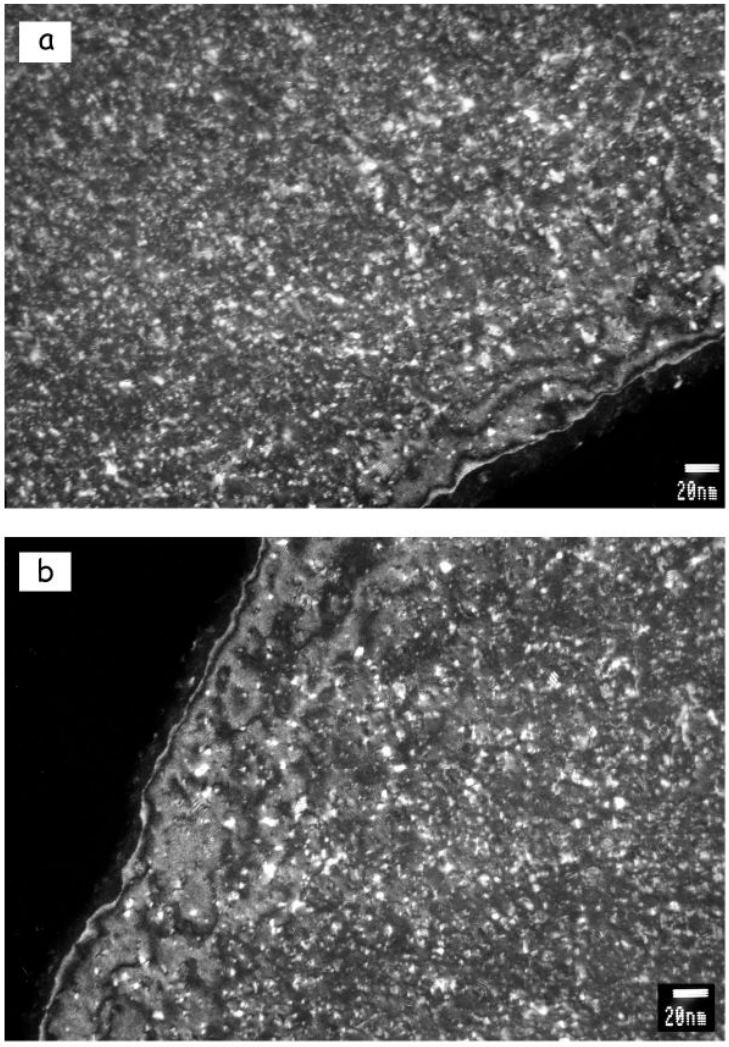

Figure 3. TEM micrographs showing precipitates and irradiation induced defect clusters in (a) prime aged (PA) and (b) overaged (HT1) Outokumpu CuCrZr alloy irradiated at 333 K to 0.3 dpa.

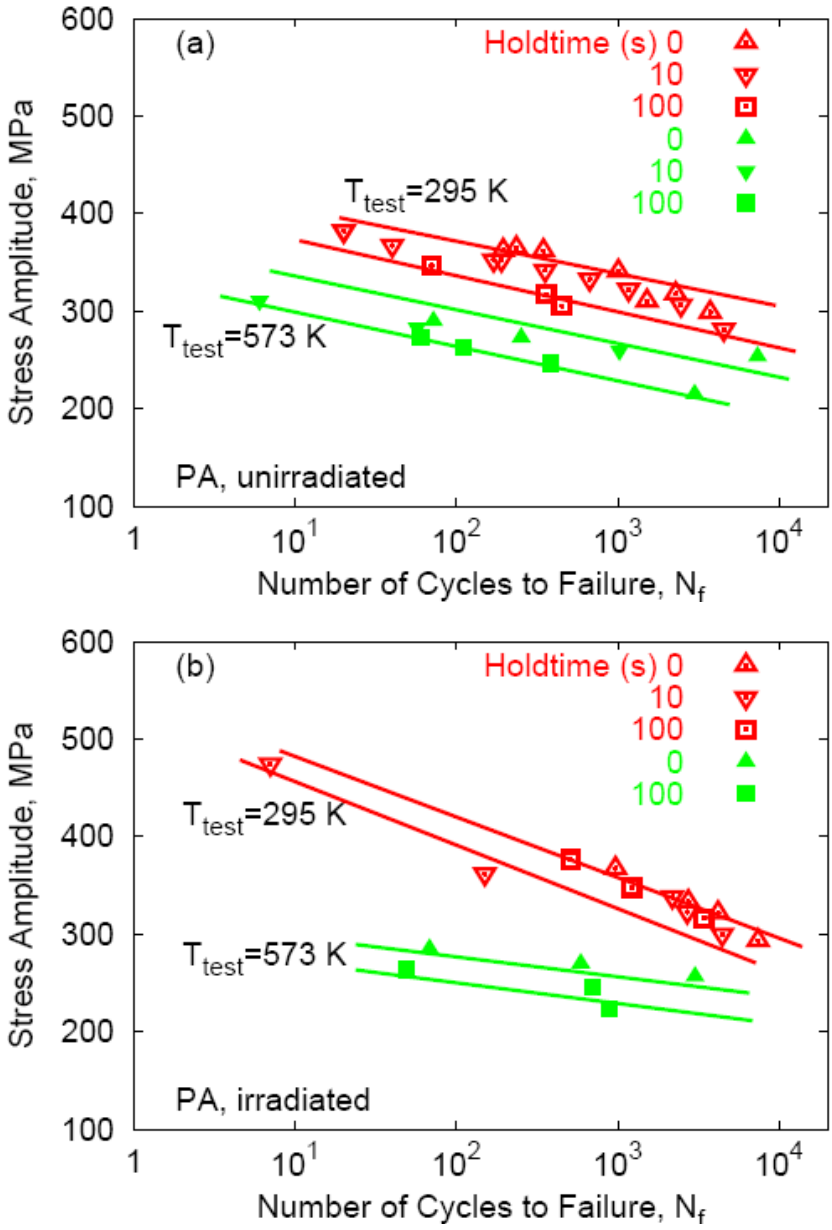

Figure 4. Variation of number of cycles to failure with stress amplitude determined using load controlled creep-fatigue tests carried out at 295 K and 573 K with different holdtimes on prime aged (PA) CuCrZr specimens in (a) unirradiated and (b) irradiated conditions. Specimens tested at 295 K and 573 K were irradiated at 333 K and 573 K, respectively, to a dose level in the range of 0.16-0.33 dpa. Tests at 573K were carried out in vacuum.

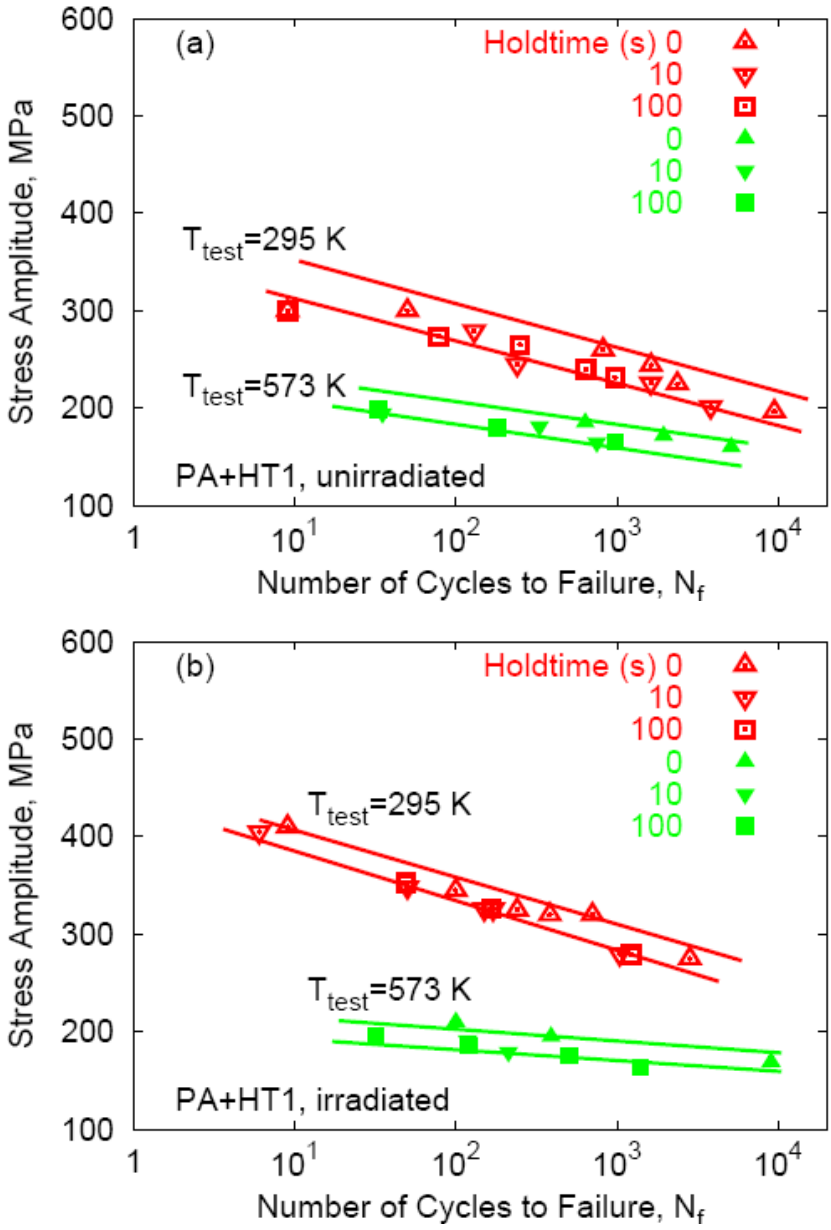

Figure 5. Same as in Figure 4 but for the overaged (HT1) CuCrZr alloy in (a) unirradiated and (b) irradiated conditions.

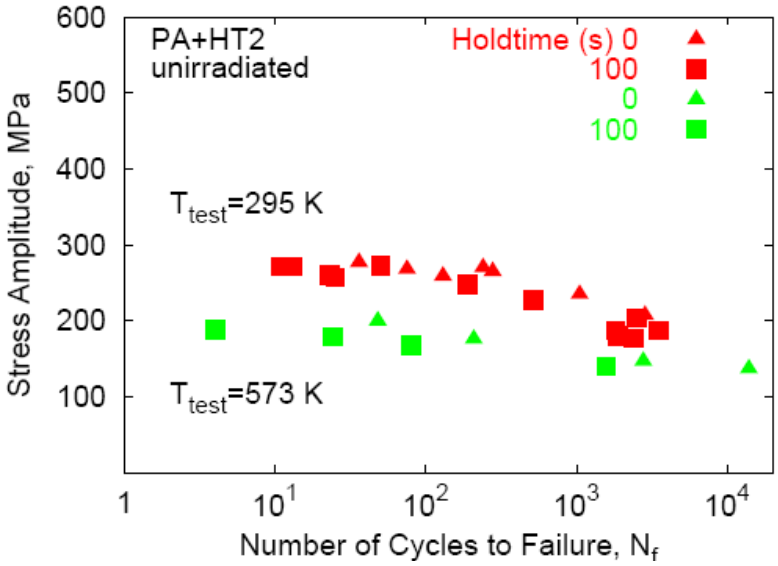

Figure 6. Same as in Figure 4 but for the overaged (HT2) CuCrZr alloy tested in the unirradiated condition at 295 and 573 K.

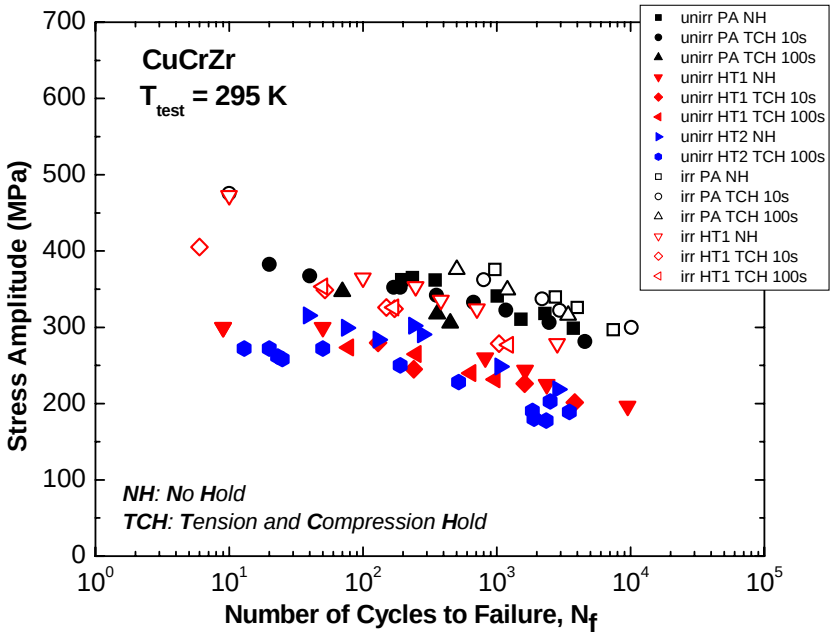

Figure 7. Dependence of the number of cycles to failure on stress amplitude determined during creep-fatigue tests in the load controlled mode at 295 K with and without holdtime. These data include the results for specimens with all heat treatments (i.e. PA, HT1 and HT2) and tested in the unirradiated as well as irradiated conditions.

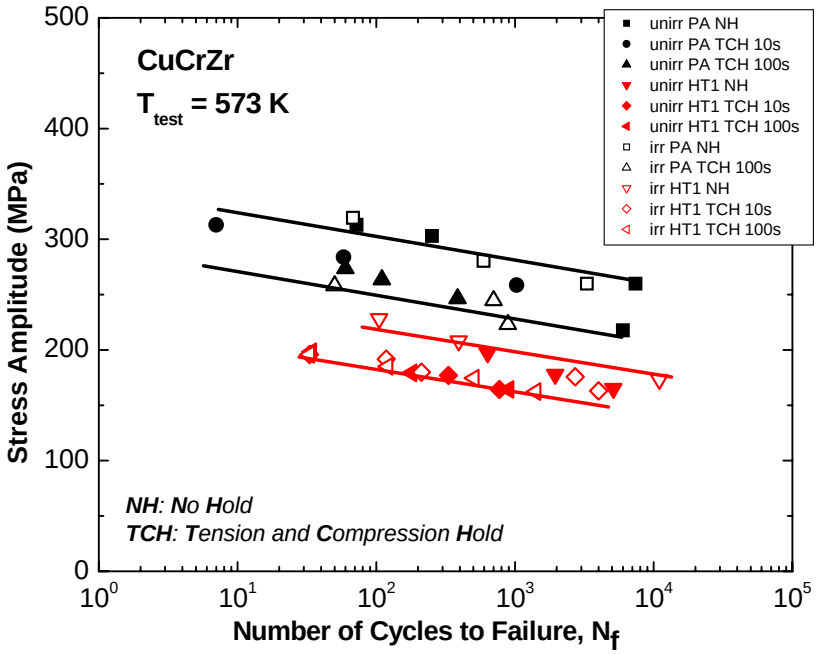

Figure 8. Same as in Figure 7 but for tests carried out at 573 K and include the results for heat treatments PA and HT1 in the unirradiated and irradiated conditions.

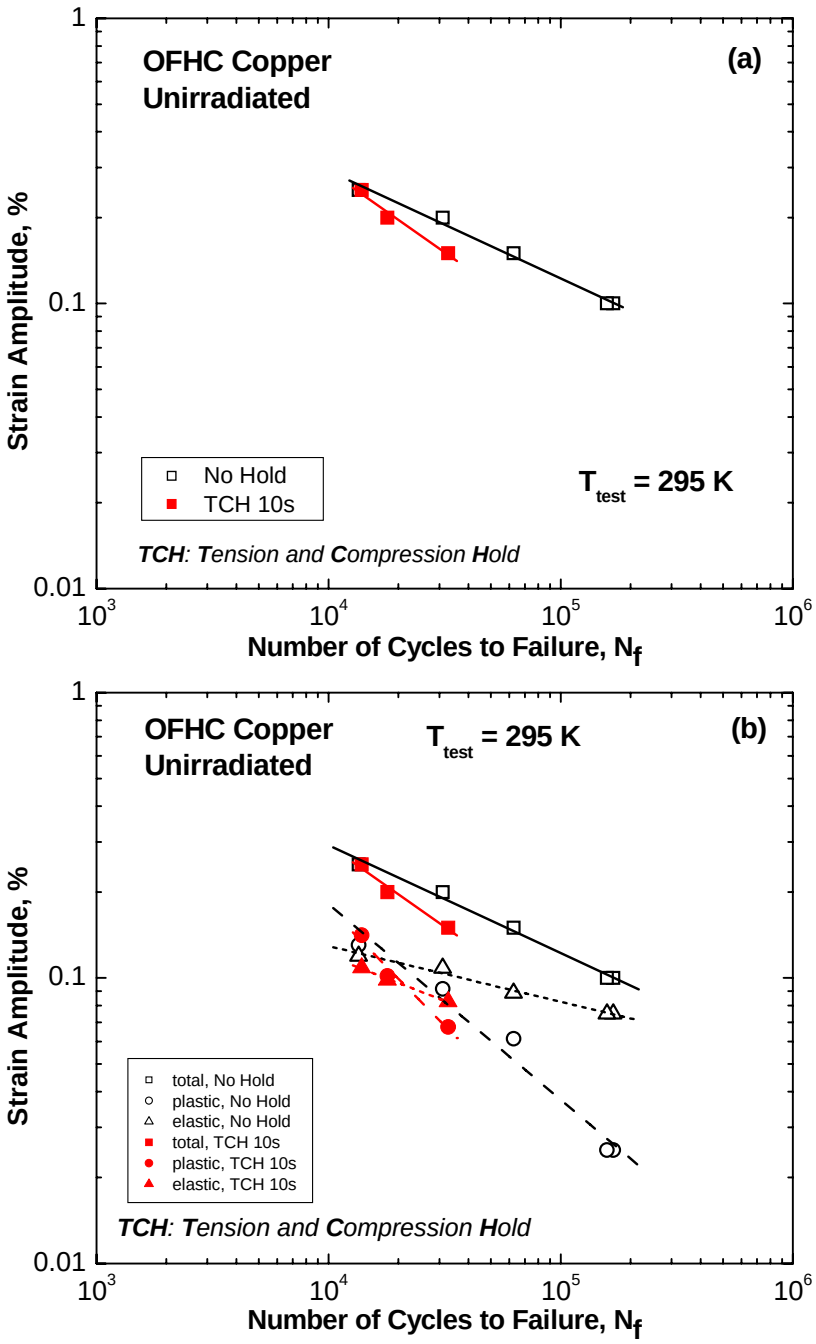

Figure 9. Strain amplitude dependence of number of cycles to failure for fully annealed OFHC-copper determined at 295 K during creep-fatigue tests carried out in the strain controlled mode: (a) shows the dependence in terms of total strain amplitude and (b) the dependence on the elastic and plastic components of the total strain.

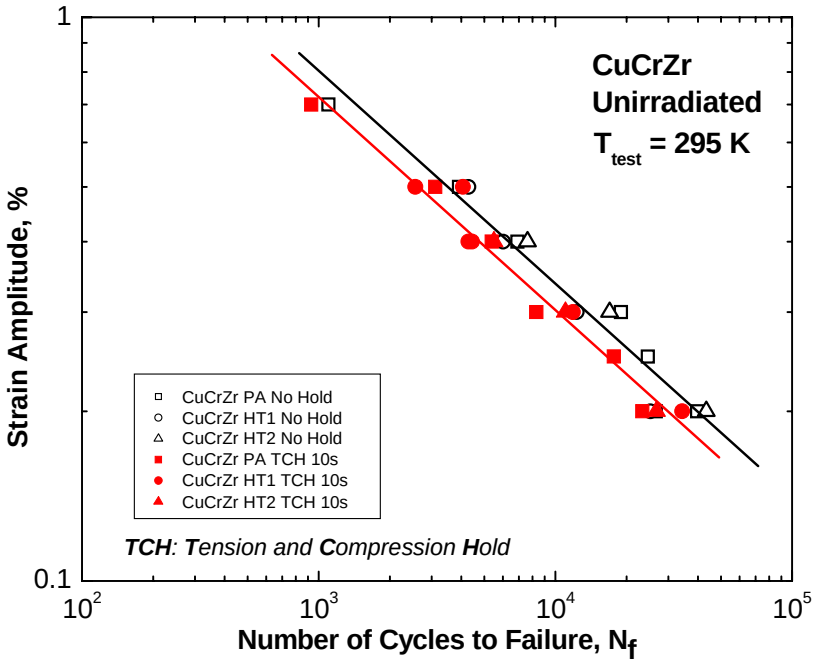

Figure 10. Same as in Figure 9 but for CuCrZr alloy with different heat treatments (i.e. PA, HT1 and HT2) tested at 295 K in strain controlled mode and in the unirradiated condition with no holdtime and a holdtime of 10 seconds.

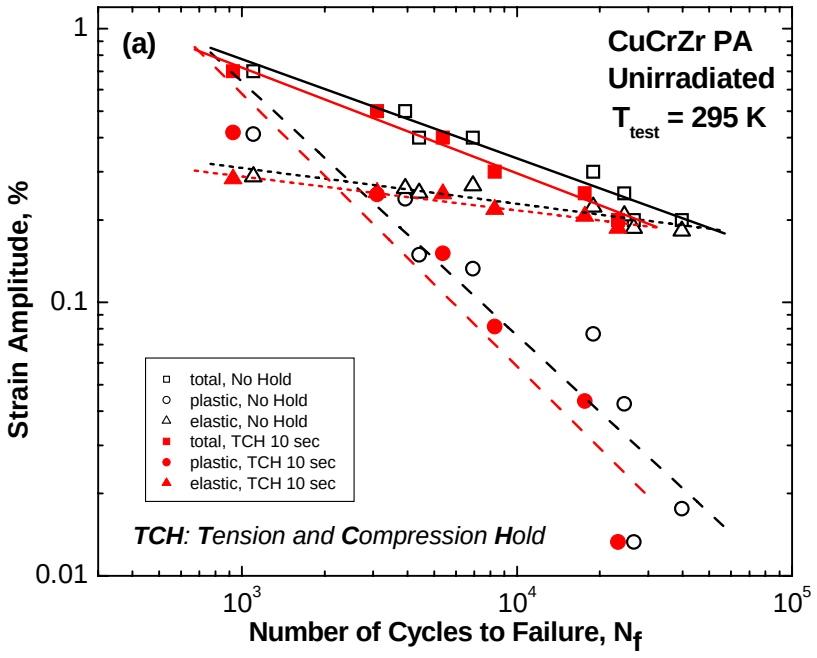

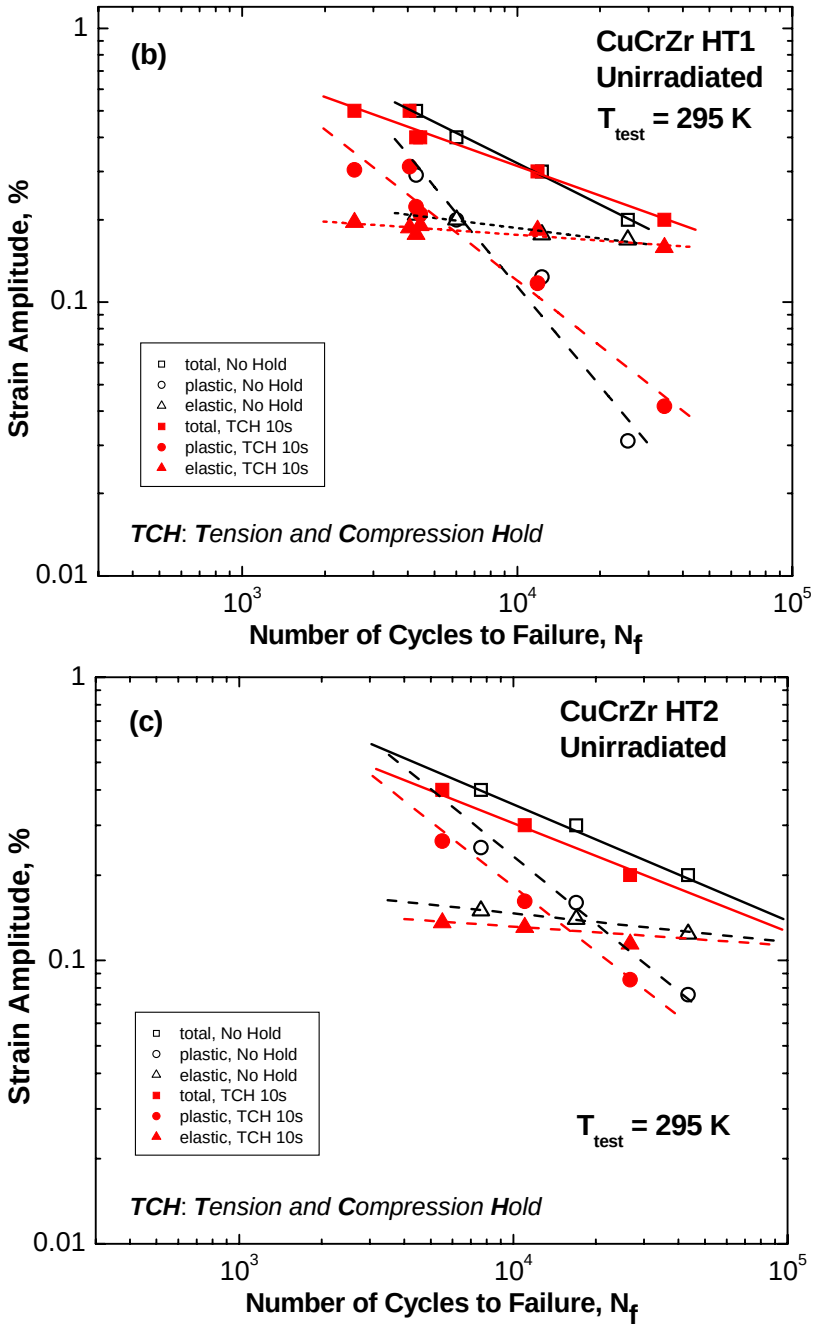

Figure 11. Number of cycles to failure obtained in the strain controlled tests as a function of elastic, plastic and total strain range for (a) PA, (b) HT1 and (c) HT2 conditions tested at 295 K with no holdtime and a holdtime of 10 seconds.

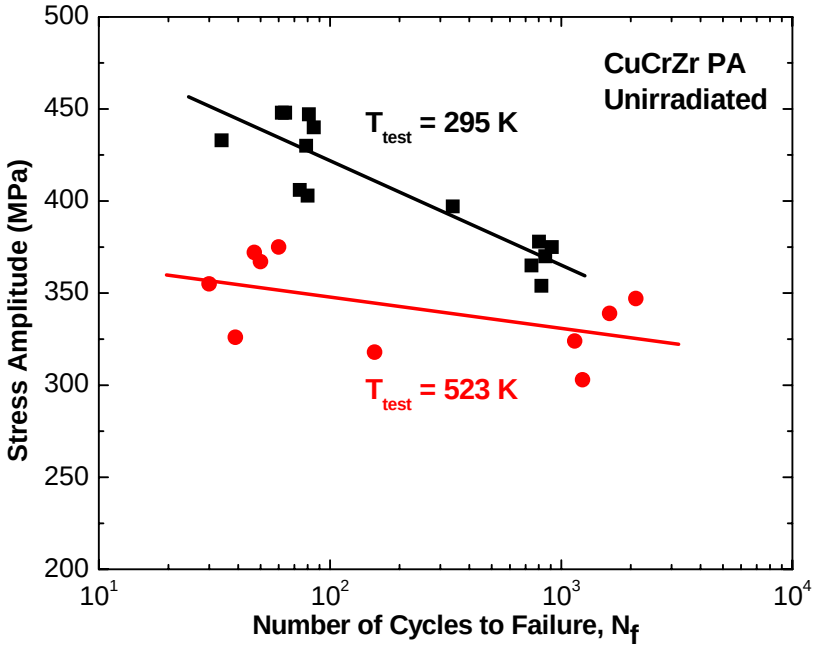

Figure 12. Number of cycles to failure obtained on the prime aged (PA) CuCrZr in the balanced load, extension controlled tests as a function of stress amplitude for all the holdtime conditions. The data includes the results of tests carried out at 295 K and 523 K with different holdtimes in the range of 2 to 1000 seconds.

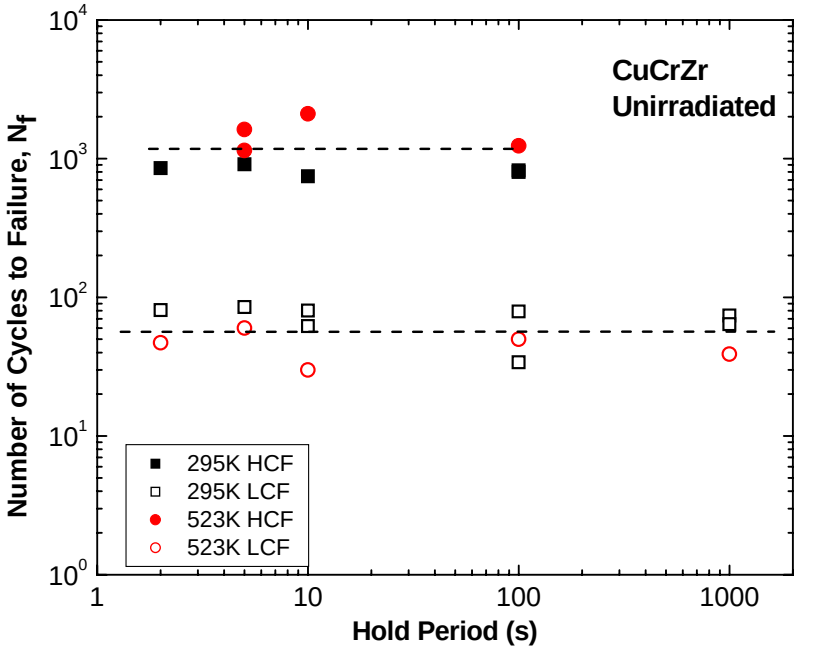

Figure 13. Effect of holdtime on the number of cycles to failure, N_f, for tests carried out at 295 K and 523 K on CuCrZr (PA) specimens. Note that data shown in this figure are for the same set of experiments used in Figure 12.

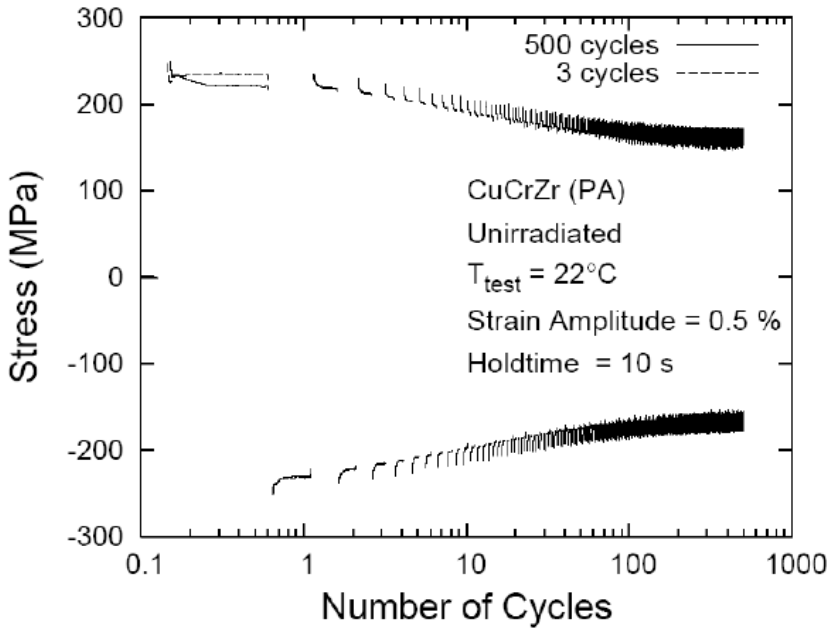

Figure 14. Number of cycles as a function of stress amplitude in "interrupted" creep-fatigue tests carried out on CuCrZr (PA) specimens in the strain controlled mode at 295 K with a total strain amplitude of 0.5% and a holdtime of 10 seconds.

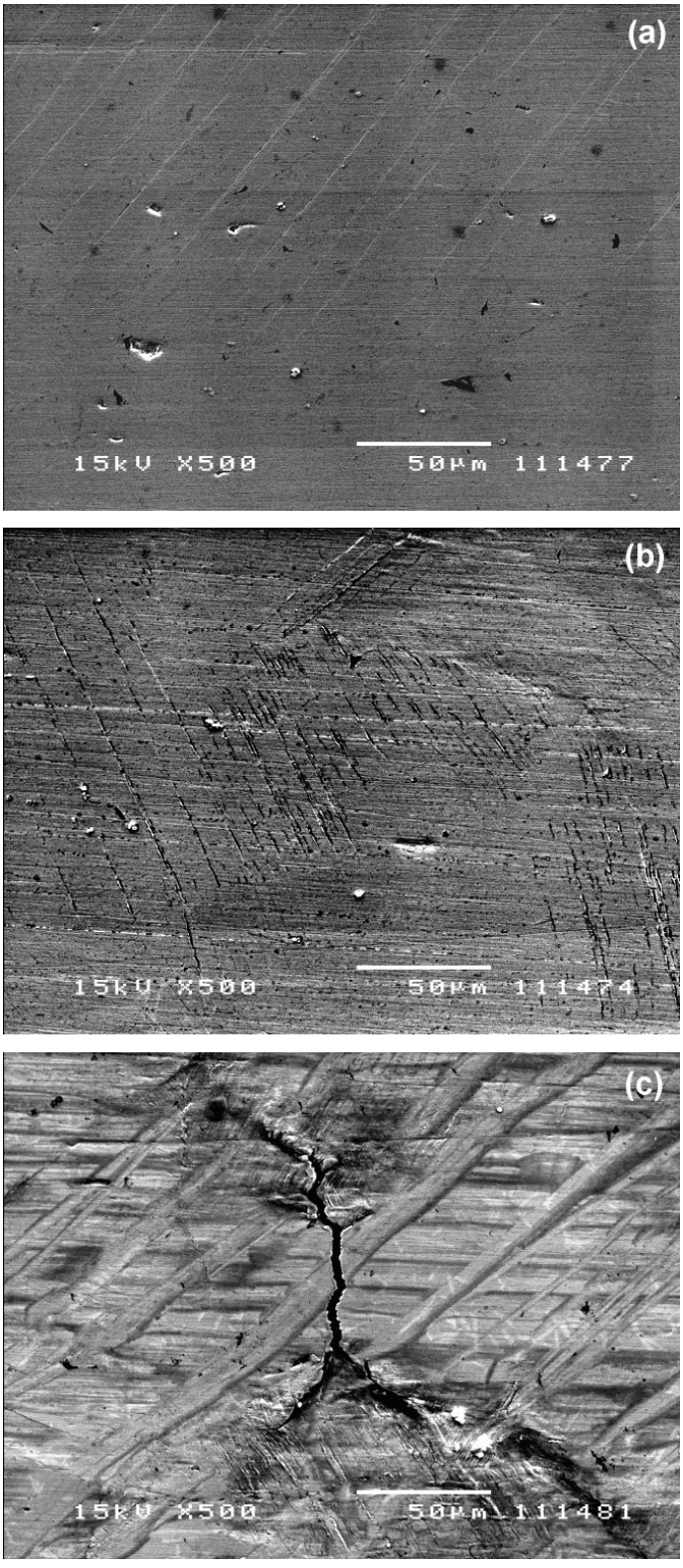

Figure 15. Scanning electron microscope (SEM) images showing slip steps at the surface of the CuCrZr (PA) specimens tested to different number of cycles: (a) 1, (b) 25 and (c) 500 cycles. Note that the slip steps appear already after the first cycle and the number increases with increasing number of cycles. At the end of 500 cycles clearly risible crack is formed (Figure 15c). These specimens were examined in transmission electron microscope and the results are shown in Figure 16.

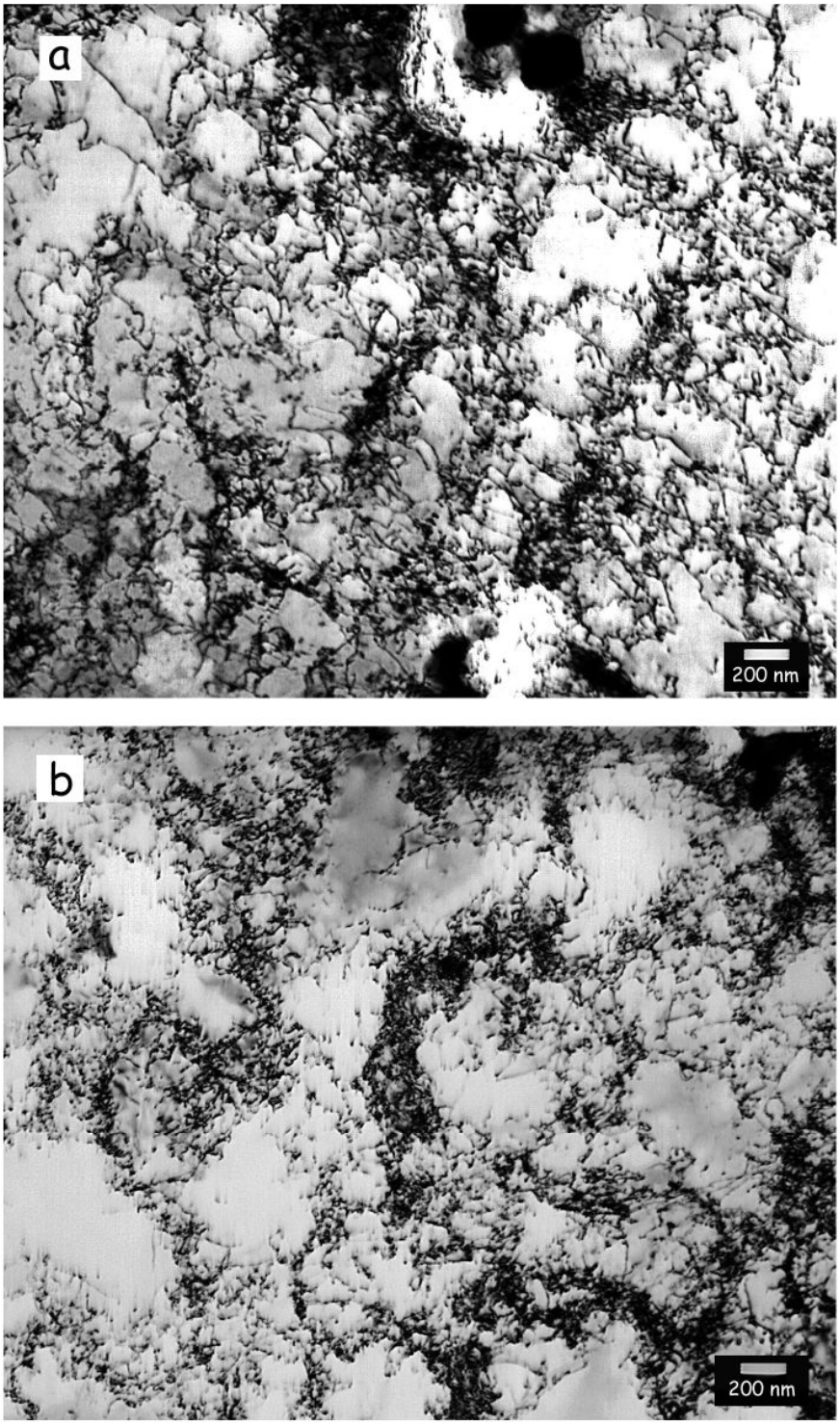
a
200 nm
b
200 nm

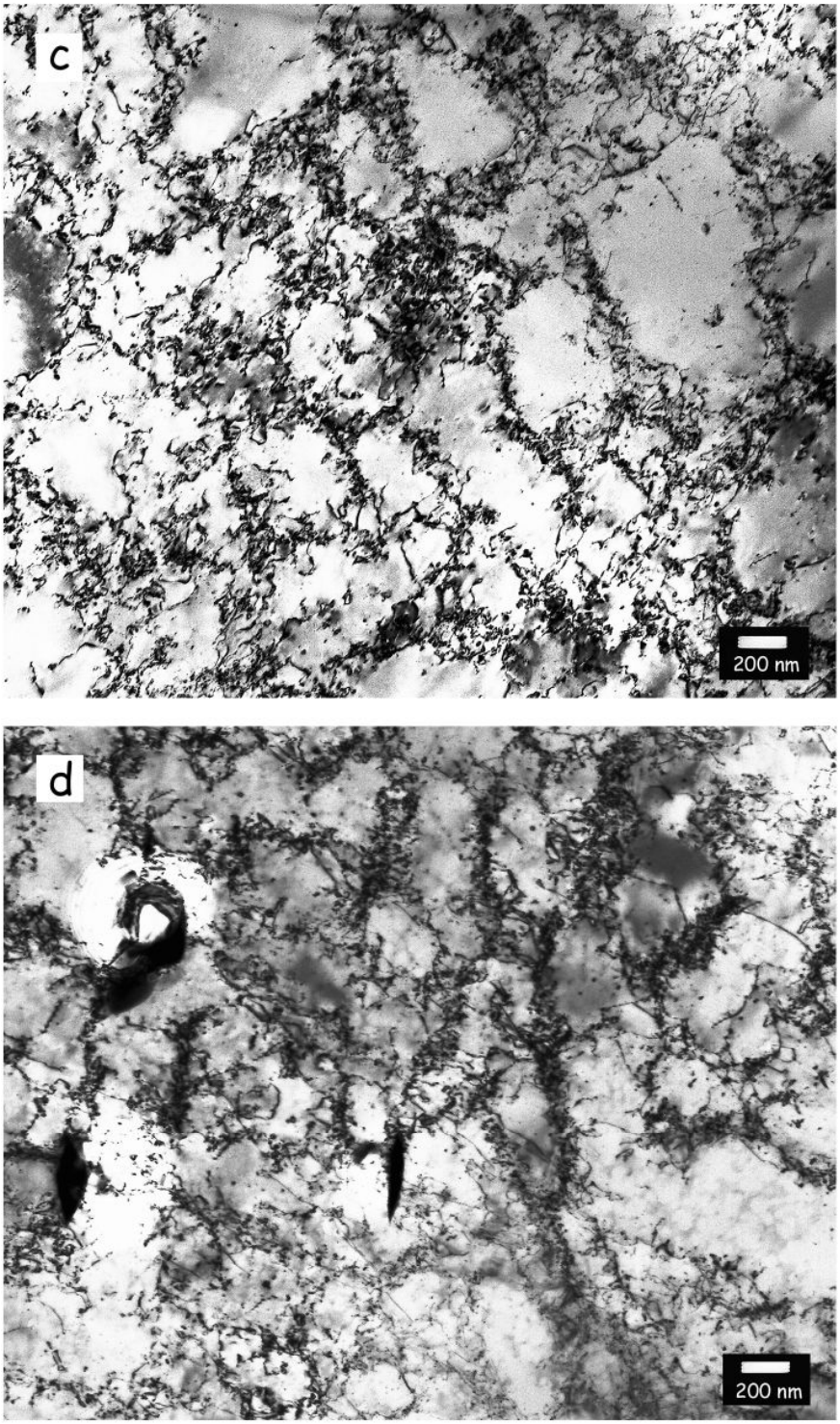
c
200 nm
d
200 nm

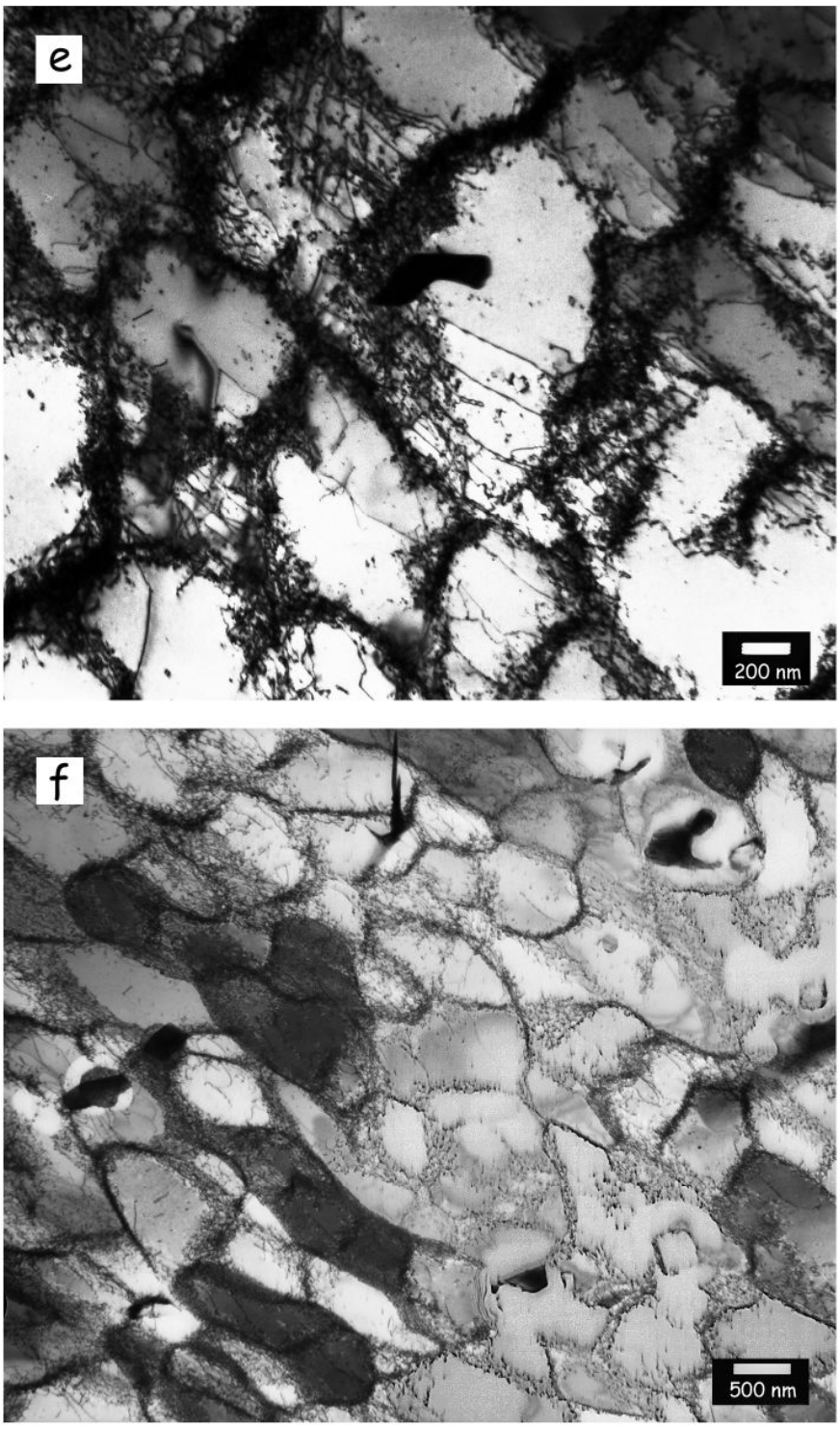

Figure 16. Transmission electron micrographs showing the evolution of dislocation microstructure during "interrupted" creep-fatigue tests carried out on CuCrZr (PA) speciemns in the strain controlled mode with a strain amplitude of 0.5% and a holdtime of 10 seconds at 295 K to different number of cycles: (a) 1, (b) 2, (c) 5, (d) 25, (e) 100 and (f) 500 cycles. Note that a high density of homogeneously distributed dislocations is formed already at the end of the first cycle. As the number of cycle increases, the dislocations begin to segregate in the form of dislocation walls and cell-like structure and by the end of 500 cycles practically no free dislocations are left (Figure 16f).

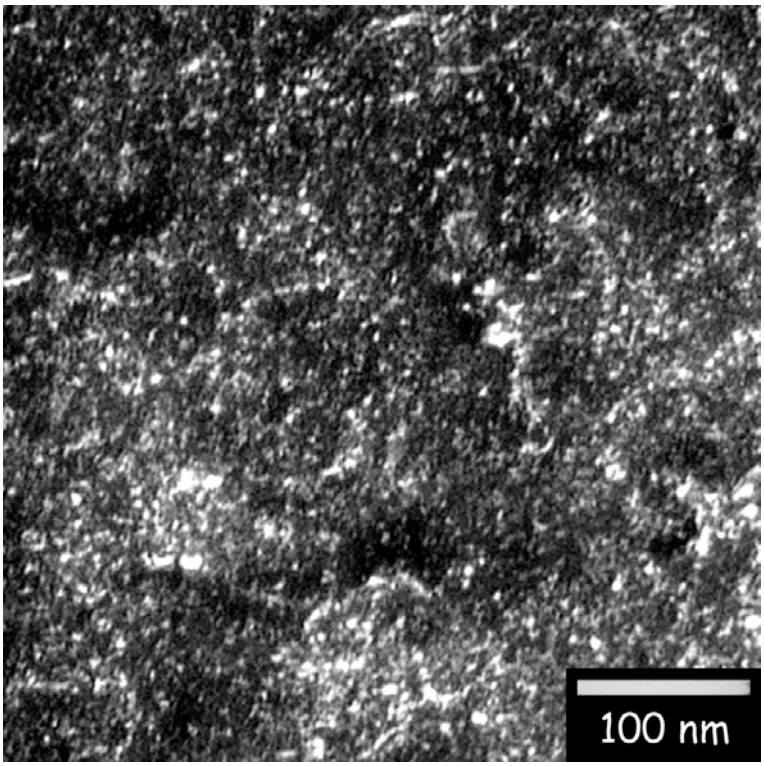

Figure 17. A transmission electron micrograph showing high density of precipitates and irradiation induced defects in the prime aged CuCrZr specimen creep-fatigue tested in post-irradiation condition at 295 K to 1200 cycles with a holdtime of 100 seconds at a stress amplitude of 350 MPa. Note that the density of precipitates and defect clusters have survived 1200 cycles of creep-fatigue deformation and their spatial distribution has remained reasonably homogeneous (compare with Figure 3).

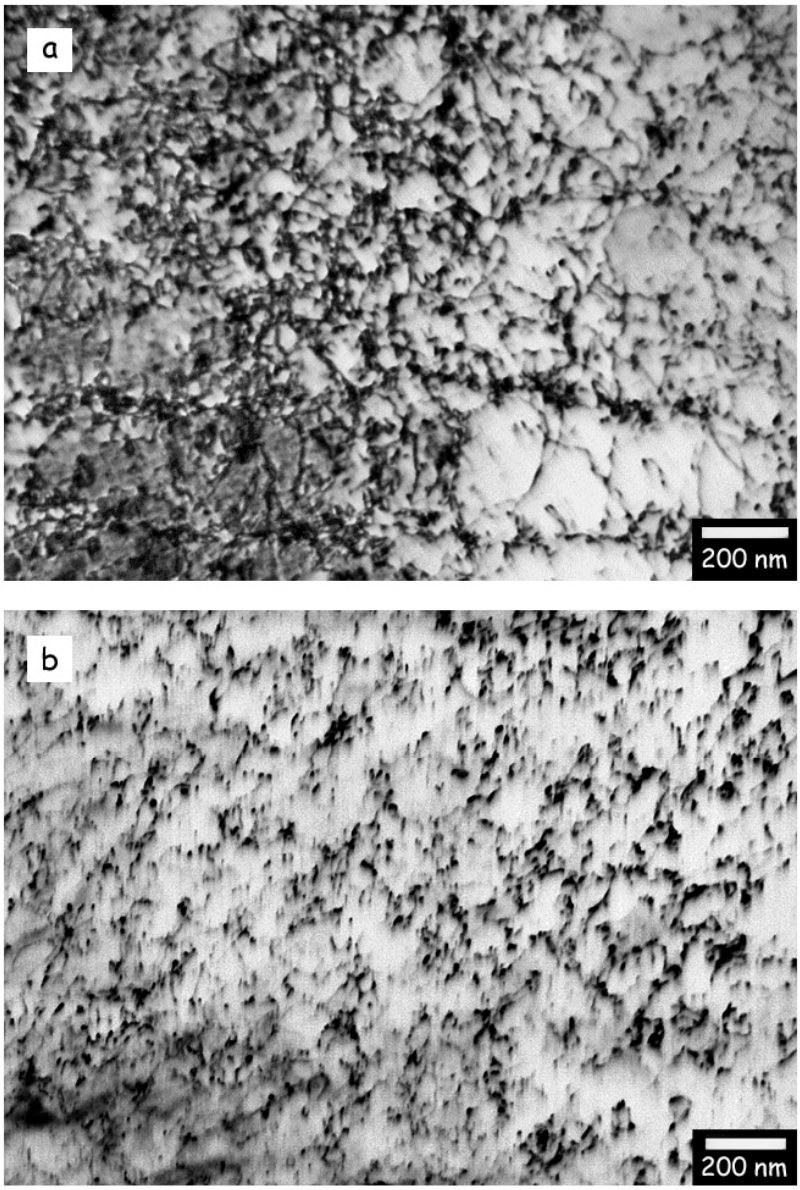

Figure 18. Transmission electron micrographs showing dislocation microstructure in the prime aged CuCrZr specimens creep-fatigue tested in the load controlled mode at 573 K in the post-irradiation condition (T_{irr}=573 K to a dose of ~0.3 dpa) with (a) no holdtime as (b) a holdtime of 100 seconds using stress amplitudes of 280 MPa and 245 MPa, respectively. The number of cycles to failure obtained in these experiments were 594 and 700 cycles, respectively.

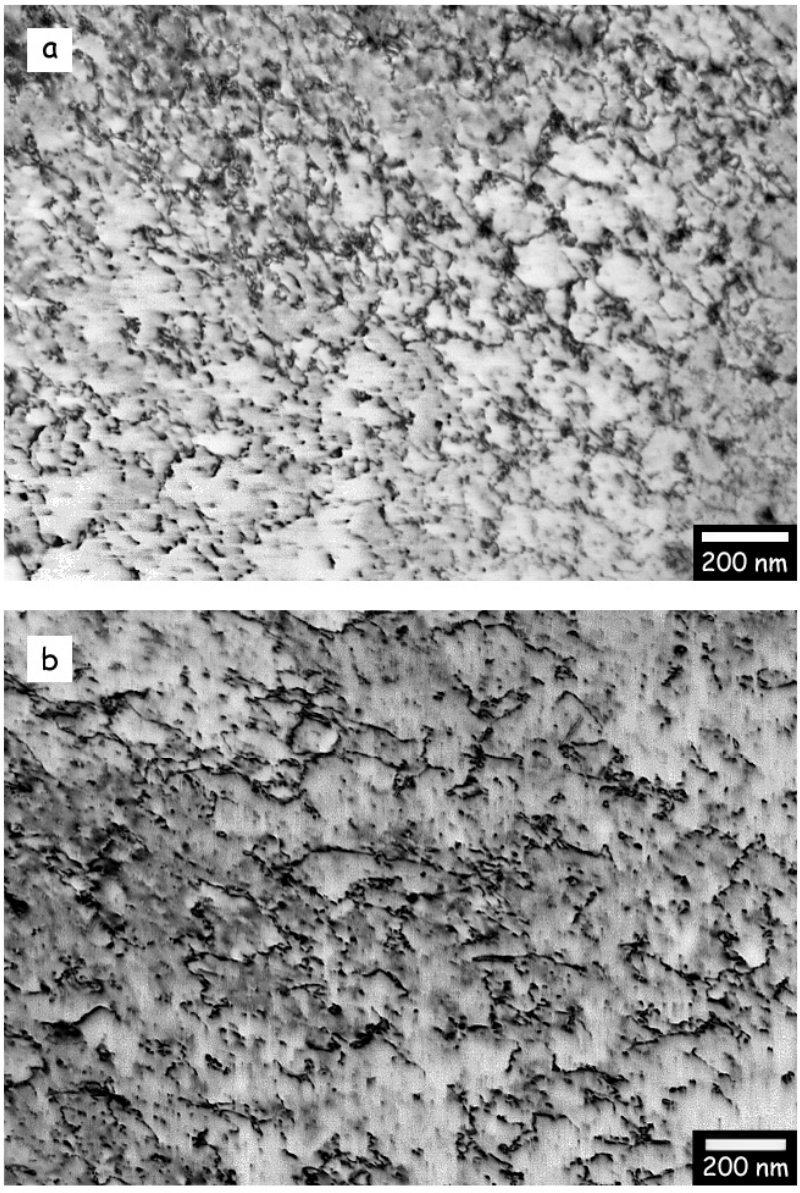

Figure 19. Same as in Figure 18 but for the overaged (HT1) CuCrZr specimens irradiated and tested at 573 K (to a dose level of ~0.3 dpa) in the load controlled mode (a) with no holdtime and (b) with a holdtime of 100s using stress amplitudes of 210 MPa and 175 MPa. The number of cycles to failure obtained in these experiments were 393 and 505 cycles, respectively.

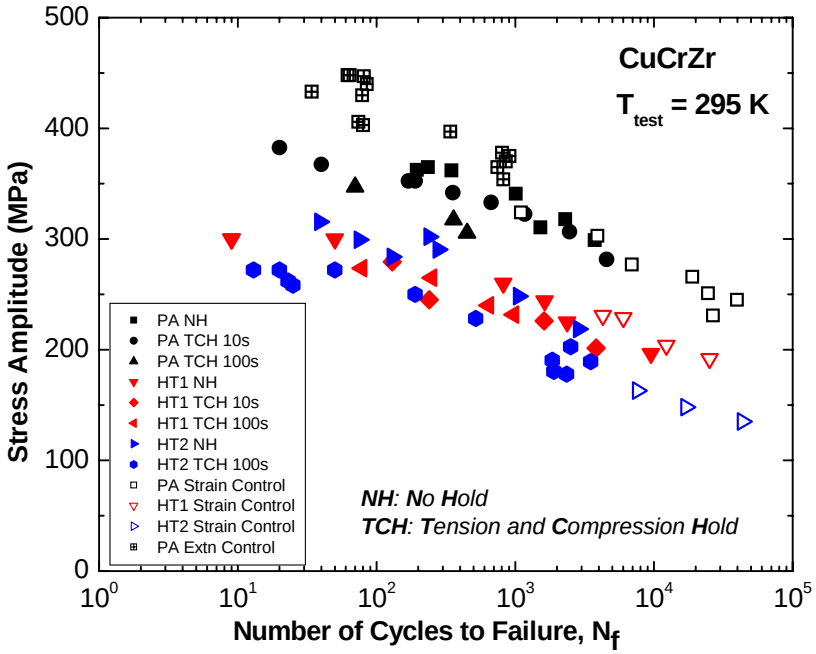

Figure 20. Comparison of all of the room temperature fatigue life data for CuCrZr PA, HT1 and HT2 for all three test conditions (i.e. load controlled, strain controlled and extension controlled).

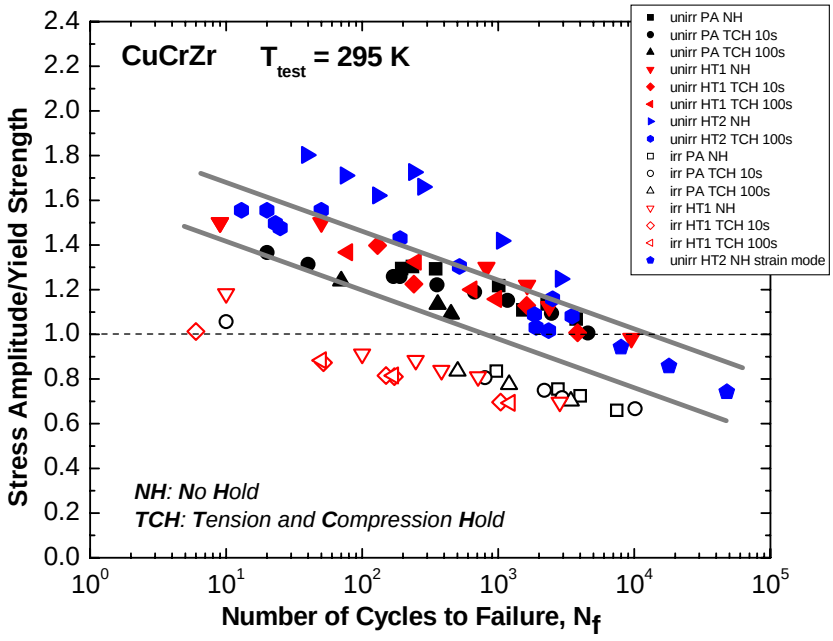

Figure 21. Fatigue lives for room temperature tests on CuCrZr (PA,HT1 and HT2) specimens shown as a function of stress amplitude normalized with respect to yield strength. The data plotted here include the results of tests carried out on specimens with different heat treatments for different holdtimes in unirradiated and irradiated conditions.

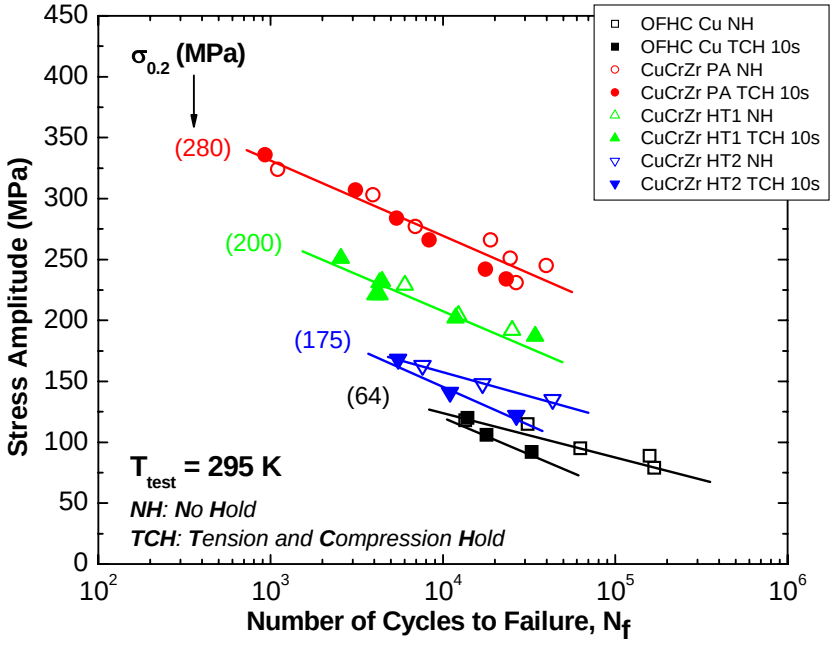

Figure 22. Number of cycles to failure (N_f) as a function of stress amplitude for OFHC-copper and CuCrZr alloy with different heat treatments (PA, HT1 and HT2) tested at 295 K in the strain controlled mode with and without holdtime. The yield strength values for CuCrZr alloy are taken from Table 2 and for OFHC-copper from Ref. [7].

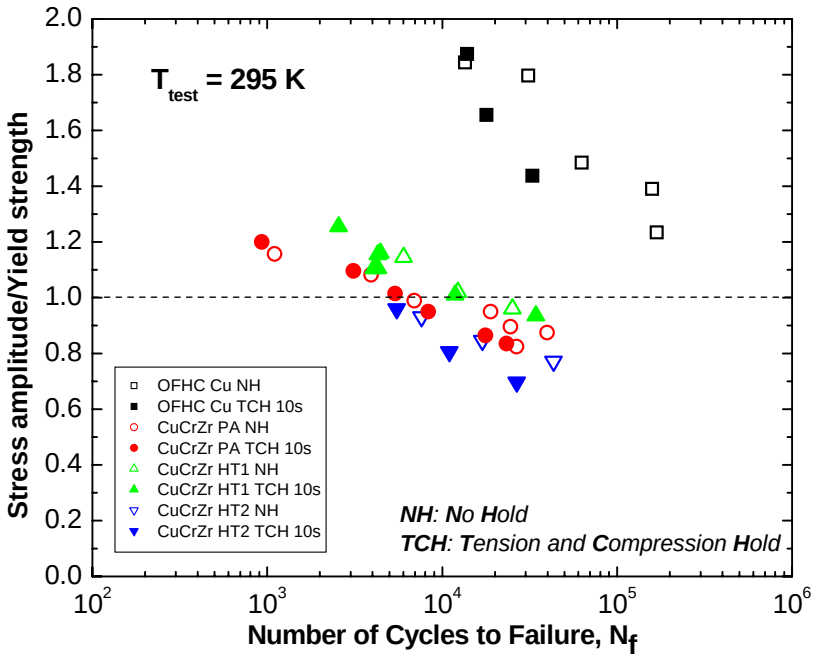

Figure 23. The lifetime (N_f) results shown in Figure 22 are replotted as a function of stress amplitude normalized with respect to yield strength. Note the segregation of lifetime values for CuCrZr alloy and OFHC-copper in two well separated blocks.

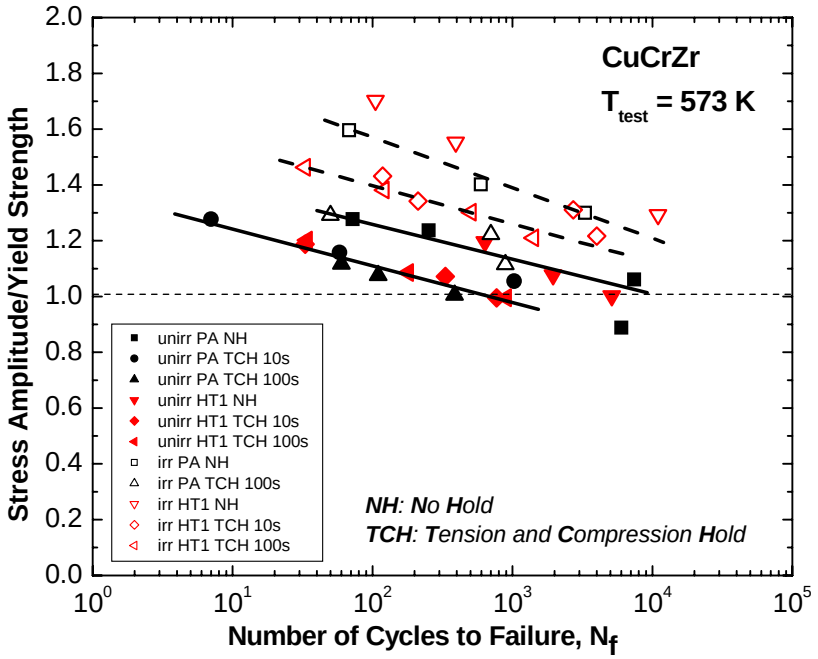

Figure 24. Same as in Figure 21 but for the tests carried out at 573 K both in the unirradiated and irradiated conditions.

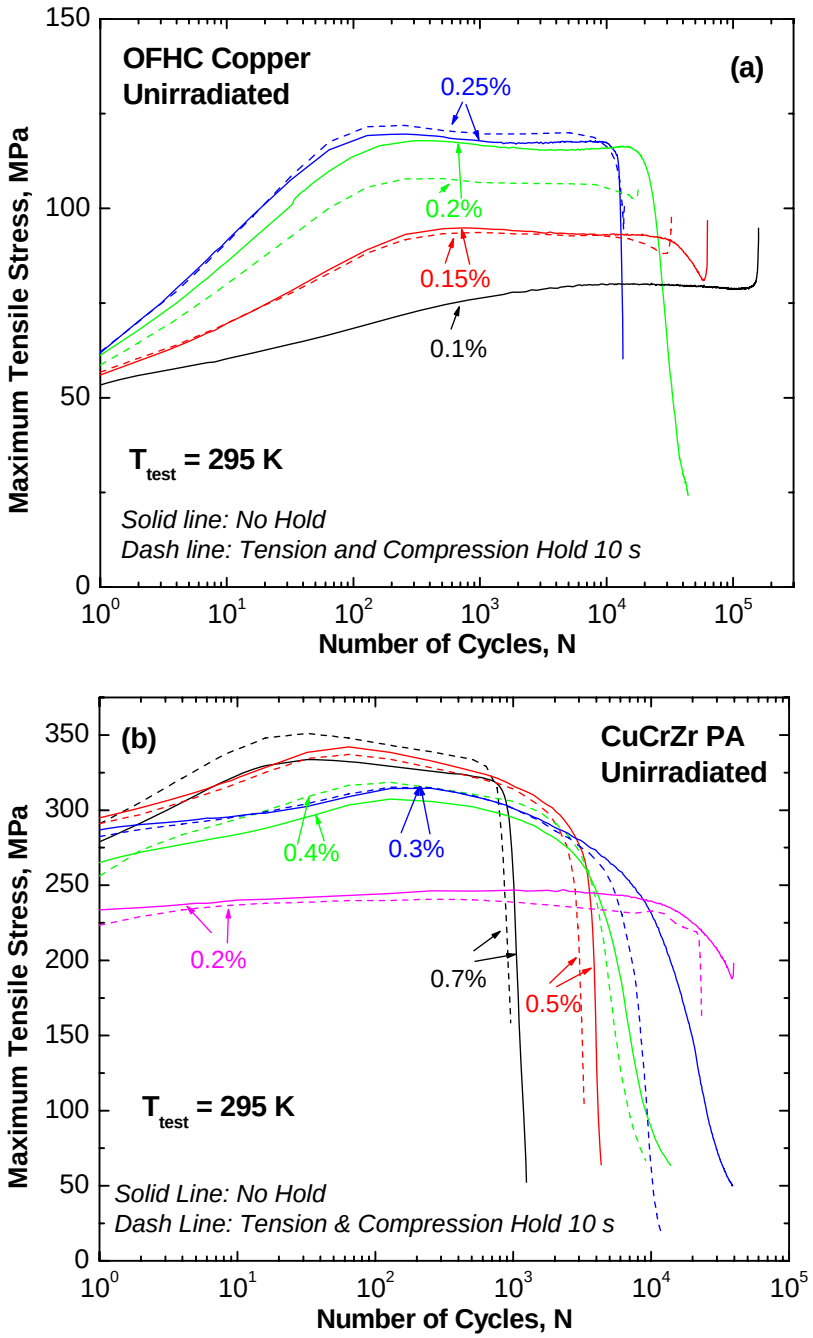
OFHC Copper
Unirradiated
(a)
0.25%
0.2%
0.15%
0.1%
T test = 295 K
Solid line: No Hold
Dash line: Tension and Compression Hold 10 s
Maximum Tensile Stress, MPa
Number of Cycles, N
(b)
CuCrZr PA
Unirradiated
0.4%
0.3%
0.2%
0.7%
0.5%
T test = 295 K
Solid Line: No Hold
Dash Line: Tension & Compression Hold 10 s
Maximum Tensile Stress, MPa
Number of Cycles, N

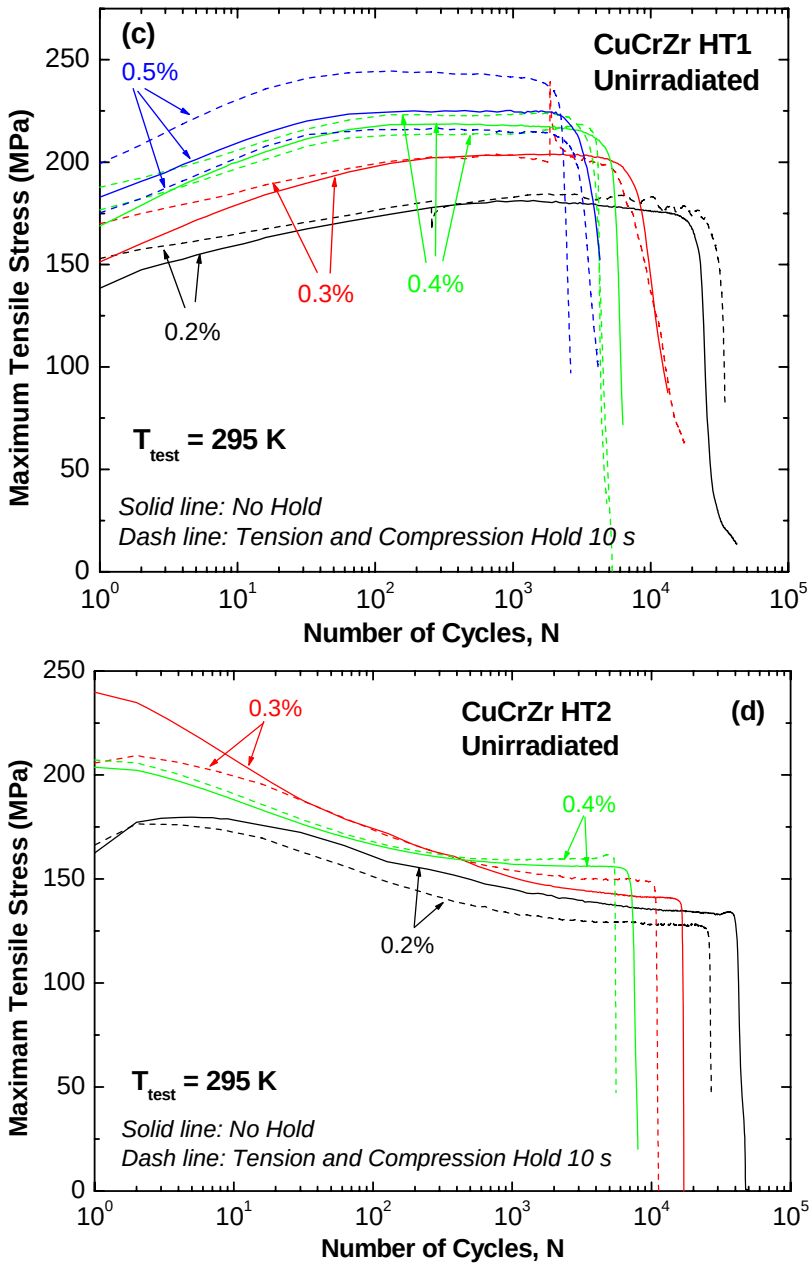

Figure 25. Maximum tensile stress as a function of number of cycles determined during strain controlled creep-fatigue tests carried out at 295 K without holdtime and with a holdtime of 10 seconds at different levels of strain amplitude for (a) OFHC-copper and CuCrZr alloy in (b) PA, (c) HT1 and (d) HT2 conditions. Note that the hardening behaviour of OFHC-Cu is substantially different from that exhibited by the CuCrZr alloy with different heat treatments. The CuCrZr specimens with heat treatment HT2 generally show softening instead of hardening.

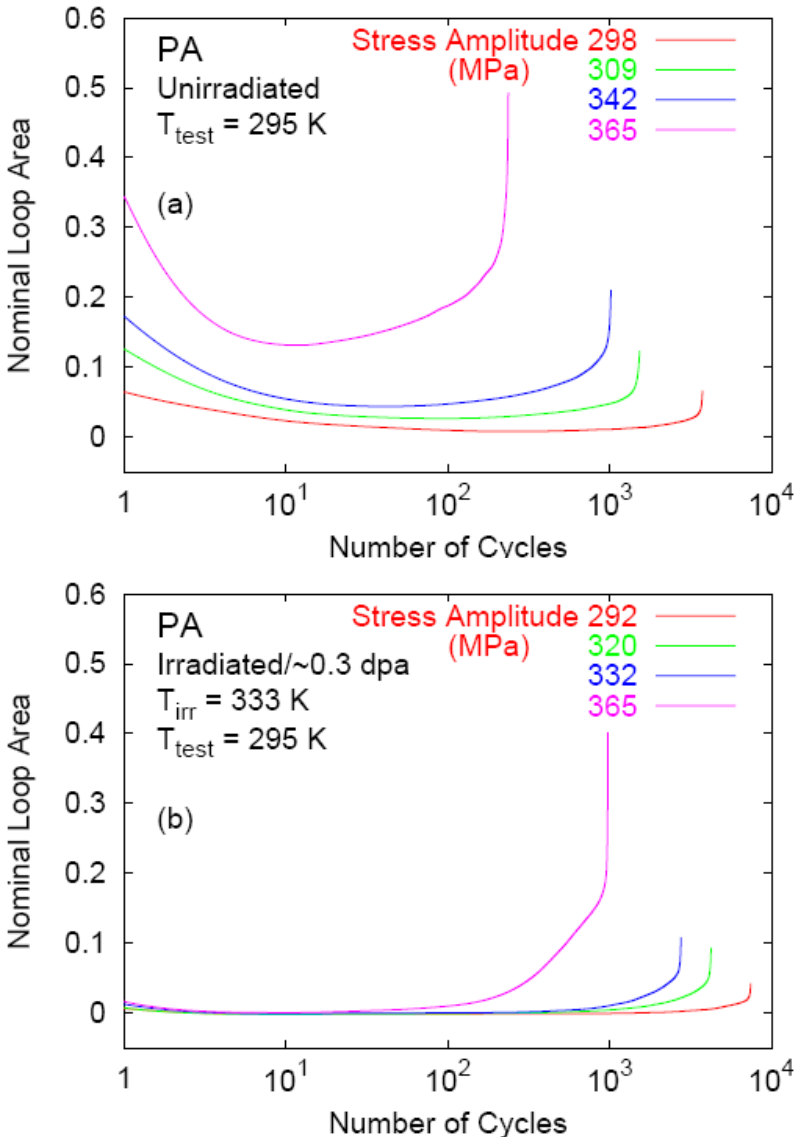

Figure 26. Nominal fatigue loop area as a function of number of cycles determined during load controlled creep-fatigue tests carried out at 295 K with different stress amplitude on CuCrZr specimens in the prime aged (PA) condition (a) before the irradiation and (b) after irradiation at 333 K to ~0.3 dpa. Note that the decrease in the loop area represents hardening. It is interesting that the irradiated specimens do not show any indication of hardening during the test.

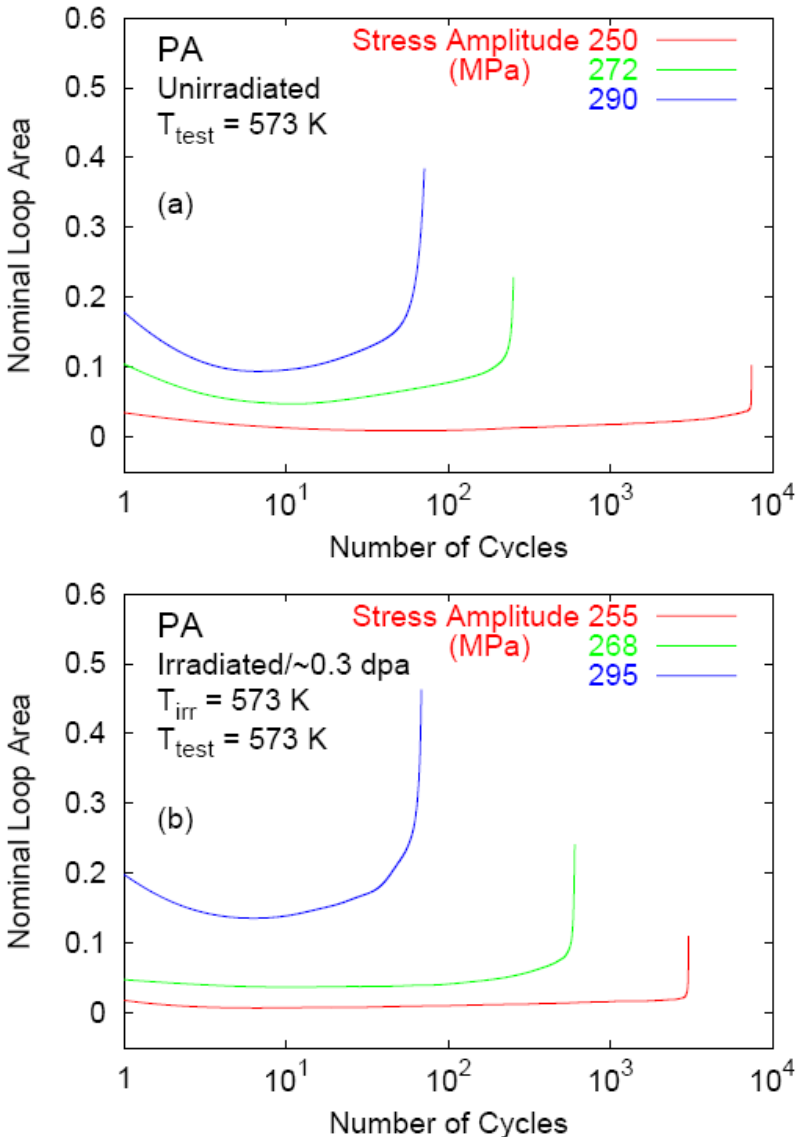

Figure 27. Same as in Figure 26 but for tests carried out at 573 K in the (a) unirradiated (b) irradiated conditions. Irradiation was carried out at 573 K to ~0.3 dpa. Note the difference in hardening behaviour between tests carried out at 295 K and 573 K.

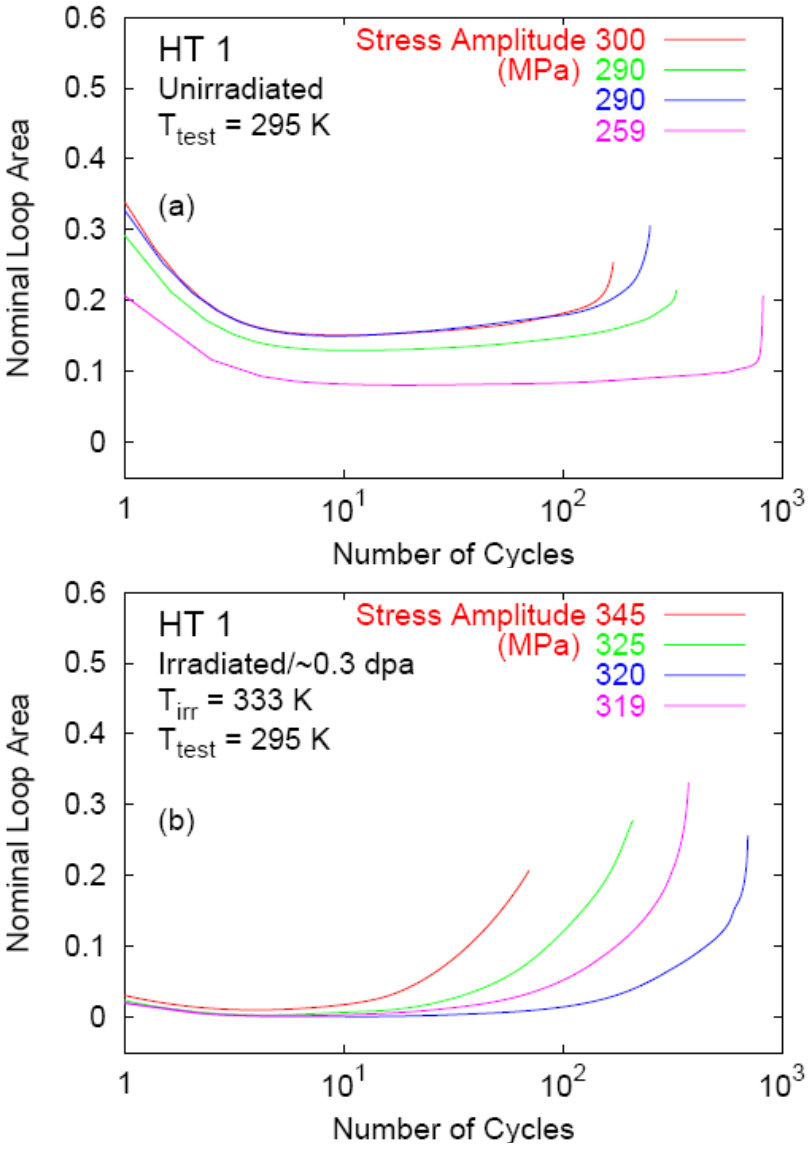

Figure 28. Same as in Figure 26 but for CuCrZr specimens tested in the overaged (HT1) condition at 295 K (a) before irradiation and (b) after irradiation at 333 K to ~0.3 dpa.

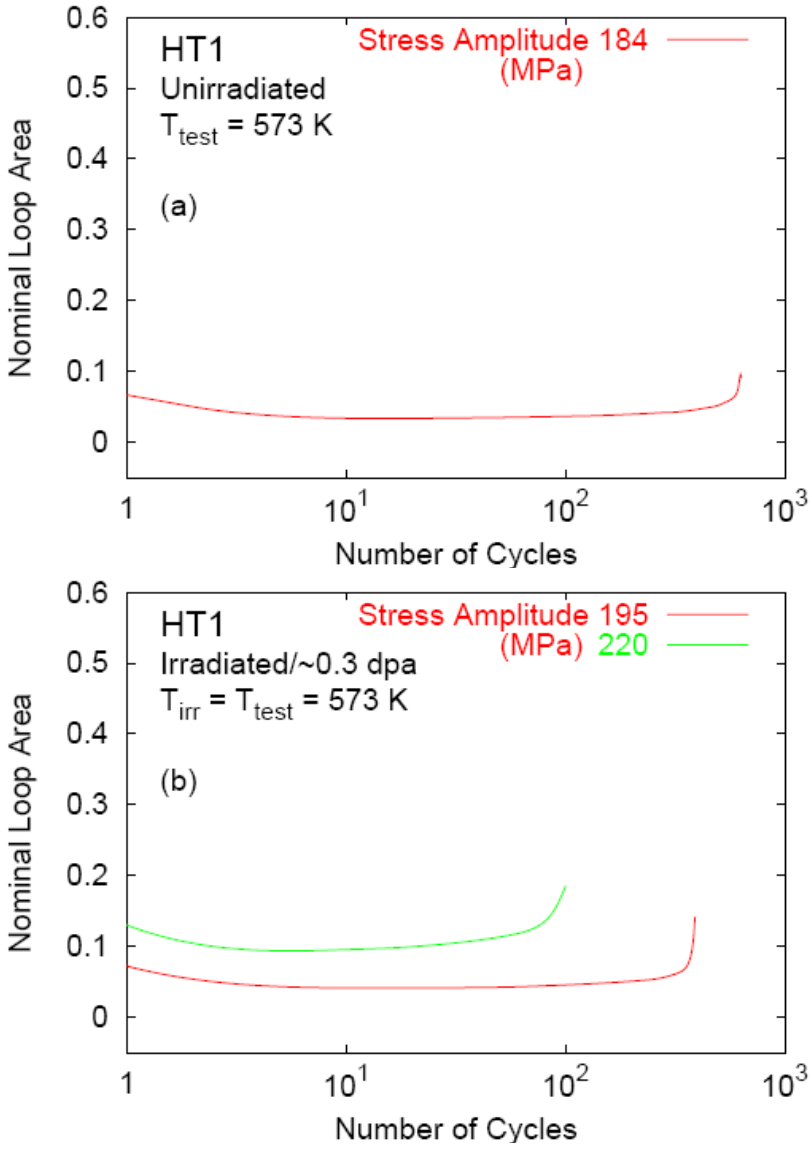

Figure 29. Same as in Figure 28 but for tests carried out at 573 K in the (a) unirradiated and (b) irradiated conditions. Irradiation was carried out at 573 K to a dose level of ~0.3 dpa. Note the lack of hardening both in the unirradiated and the irradiated conditions.

Mission

To promote an innovative and environmentally sustainable technological development within the areas of energy, industrial technology and bioproduction through research, innovation and advisory services.

Vision

Risø's research **shall extend the boundaries** for the understanding of nature's processes and interactions right down to the molecular nanoscale.

The results obtained shall **set new trends** for the development of sustainable technologies within the fields of energy, industrial technology and biotechnology.

The efforts made **shall benefit** Danish society and lead to the development of new multi-billion industries.